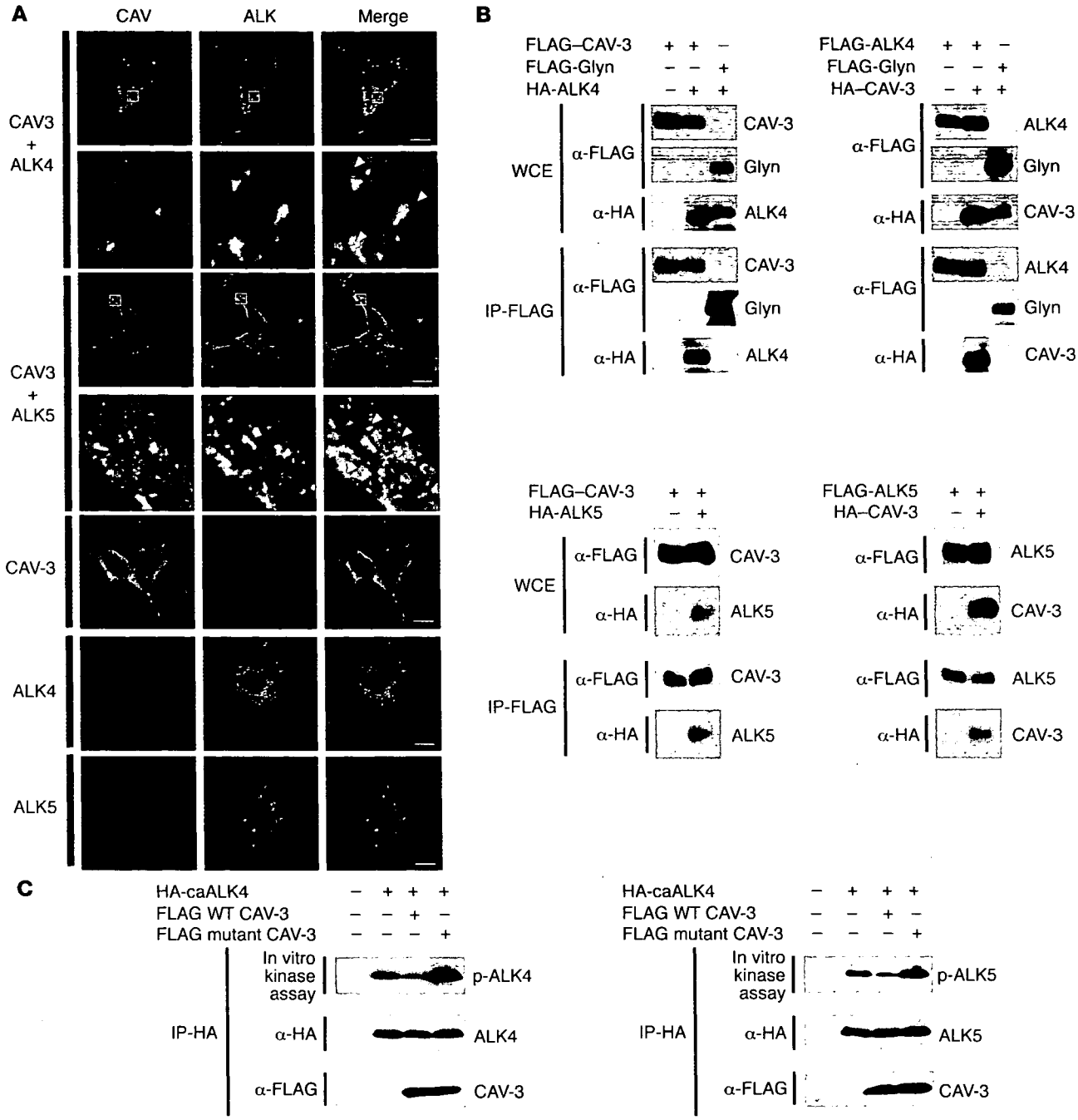

Figure 1

Caveolin-3 binds to the type I myostatin receptors and suppresses their activation. (**A**) Colocalization of caveolin-3 (CAV-3) and type I myostatin receptors (ALK4 and ALK5). COS-7 cells transfected with caveolin-3 and/or ALK4 or ALK5 were double labeled with an anti-rabbit caveolin-3 polyclonal Ab (CAV) and an anti-mouse HA mAb (ALK). The enlarged images of the boxed regions are shown below the original pictures. White arrowheads indicate colocalization of caveolin-3 with ALK4 or ALK5. Scale bars: 10 μm. (**B**) Interaction of caveolin-3 and ALK4 (upper panels) or ALK5 (lower panels). Cell lysates from COS-7 cells cotransfected with FLAG- or HA-tagged caveolin-3 (CAV-3) and either HA- or FLAG-tagged type I receptor were immunoprecipitated with anti-FLAG agarose gel, then immunoblotted using anti-FLAG mAb (α-FLAG) or anti-HA mAb (α-HA). Also, whole cell extracts (WCE) were analyzed by immunoblotting with the same Abs. Glycogenin (Glyn) was used as a negative control for immunoprecipitation. (**C**) In vitro autophosphorylation of constitutively active ALK4 and ALK5. Cell lysates from COS-7 cells cotransfected with FLAG-tagged wild-type or P104L mutant caveolin-3 and HA-tagged constitutively active ALK4 (HA-caALK4) or ALK5 (HA-caALK5) were immunoprecipitated with anti-HA agarose. The in vitro kinase reaction was initiated by the addition of kinase reaction buffer and [γ-^{32}P]ATP. Phosphorylated caALK4 or caALK5 was detected by autoradiography. Immunoprecipitated caALK4, caALK5, and caveolin-3 were analyzed by immunoblotting with anti-HA mAb (α-HA) or anti-FLAG (α-FLAG) mAb. Bands corresponding to phosphorylated type I receptor (in vitro kinase assay), total type I receptor (α-HA), and caveolin-3 (α-FLAG) are shown.

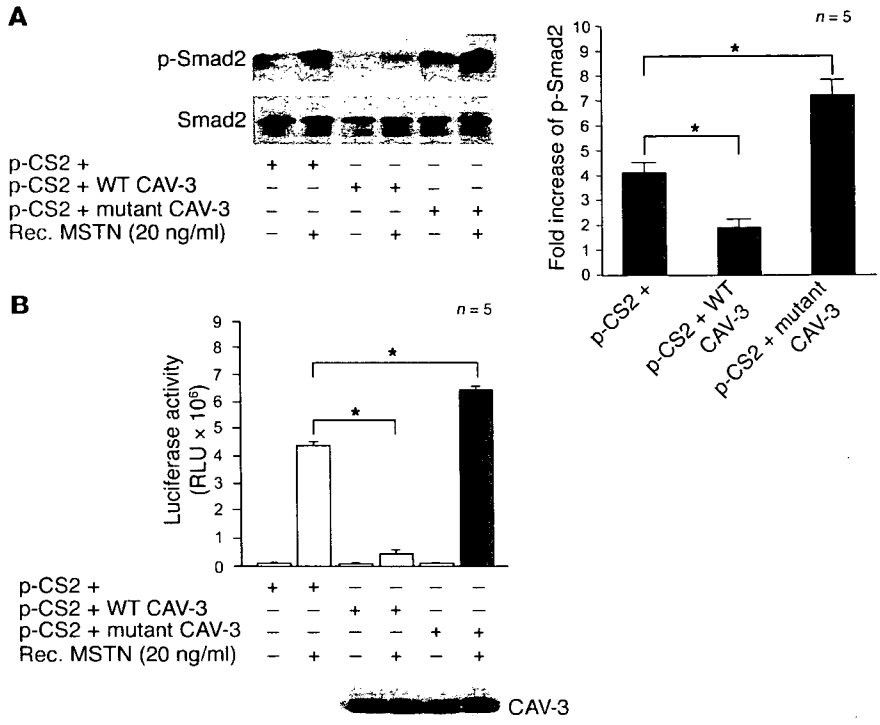

Figure 2
Caveolin-3 inhibits intracellular myostatin (MSTN) signaling in vitro. (**A**) Immunoblot analysis of total Smad2 (Smad2) and p-Smad2 in cell lysates from COS-7 cells transfected with empty vector (p-CS2+), wild-type caveolin-3 (p-CS2 + wild-type CAV-3), or P104L mutant caveolin-3 (p-CS2 + mutant CAV-3) in the presence or absence of recombinant myostatin (rec. MSTN) (left). Quantification of the fold increase of phosphorylated Smad2 in cell lysates in response to myostatin (right). Data are expressed as mean ± SD (n = 5). *P < 0.05. (**B**) Myostatin-induced luciferase activity in HEK293 cells cotransfected with a Smad-responsive reporter gene and empty vector, wild-type caveolin-3, or mutant caveolin-3. Data are expressed as mean ± SD (n = 5). *P < 0.05. Immunoblot analysis of caveolin-3 in cell lysates is shown in the lower panel.

caveolin-3 in muscle might participate in the pathogenesis of skeletal muscle atrophy in LGMD1C patients. Our caveolin-3–deficient mouse model is a useful tool for investigating how myostatin signaling is altered in LGMD1C patients. In the current study, we investigated our hypothesis by examining the interaction between caveolin-3 and type I myostatin receptor signaling in vitro. Additionally, we generated and characterized the double-Tg mice (CAV-3^{P104L}/MSTN^{Pro}) by heterozygous mating of the mutant caveolin-3–Tg mice (CAV-3^{P104L}) (5) with the mutant myostatin-Tg mice (MSTN^{Pro}) overexpressing the prodomain myostatin (12) to investigate the effect of myostatin inhibition in vivo on caveolin-3–deficient muscular atrophy. Furthermore, we injected a soluble form of type II myostatin receptor, another myostatin inhibitor (19, 24), into the mutant caveolin-3–Tg mice to investigate the therapeutic potential of myostatin inhibition for the future treatment of LGMD1C patients.

Results

Caveolin-3 can associate with the type I myostatin receptor. We first investigated whether caveolin-3 can associate with the type I myostatin receptor in vitro. COS-7 monkey kidney cells cotransfected with FLAG-tagged caveolin-3 and HA-tagged type I receptor (ALK4 or ALK5) were double immunostained with an anti-rabbit caveolin-3 polyclonal Ab and an anti-mouse mAb against HA. Confocal microscopy showed that caveolin-3 colocalized with ALK4 or ALK5 (Figure 1A). We next investigated the potential interaction of caveolin-3 with the type I myostatin receptor. COS-7 cells cotransfected with FLAG- or HA-tagged caveolin-3 and HA- or FLAG-tagged type I receptor were lysed and precipitated with anti-FLAG agarose. We detected coprecipitation of caveolin-3 with type I receptors and, conversely, type I receptors with caveolin-3 by immunoblotting with an anti-HA Ab (Figure 1B). These results indicate that caveolin-3 associates with type I myostatin receptors.

Caveolin-3 negatively regulates activation of the type I myostatin receptor. The association of caveolin-3 with type I myostatin receptor raised the intriguing possibility that caveolin-3 regulates the serine/threonine kinase activity of ALK4 or ALK5. Therefore, to determine whether caveolin-3 can affect the phosphorylation status of type I myostatin receptors, we investigated the autophosphorylation of constitutively active ALK4 or ALK5 (Figure 1C). COS-7 cells were cotransfected with HA-tagged constitutively active type I receptor and FLAG-tagged wild-type or P104L mutant caveolin-3. Constitutively active type I receptor was immunoprecipitated with anti-HA agarose and subsequently subjected to an in vitro kinase reaction. We found that phosphorylation of ALK4 or ALK5 was decreased by the wild-type caveolin-3, and conversely, increased by the P104L mutant caveolin-3 (Figure 1C). These results indicate that caveolin-3 inhibits activation of the type I myostatin receptor whereas the P104L mutant caveolin-3 enhances activation of the type I myostatin receptor in vitro.

Caveolin-3 inhibits myostatin-induced phosphorylation of Smad2. Because the activation of type I receptor induces phosphorylation of an intracellular effector, Smad2 (20, 21), we investigated whether the level of Smad2 phosphorylation is affected by caveolin-3. COS-7 cells transfected with either the wild-type or the P104L mutant caveolin-3 were stimulated with recombinant myostatin. Cell lysates were then subjected to immunoblot analysis using an Ab against Smad2 or phosphorylated Smad2 (p-Smad2). The amount of total Smad2 proteins was invariable (Figure 2A). The basal and fold increases of p-Smad2 levels were reduced in the wild-type CAV-3 transformant, but they were increased in the mutant CAV-3 transformant (Figure 2A). Thus, myostatin-induced Smad2 phosphorylation was inhibited by the wild-type caveolin-3 and, conversely, enhanced by the mutant caveolin-3, indicating that caveolin-3 regulates intracellular myostatin signaling at the effector level.

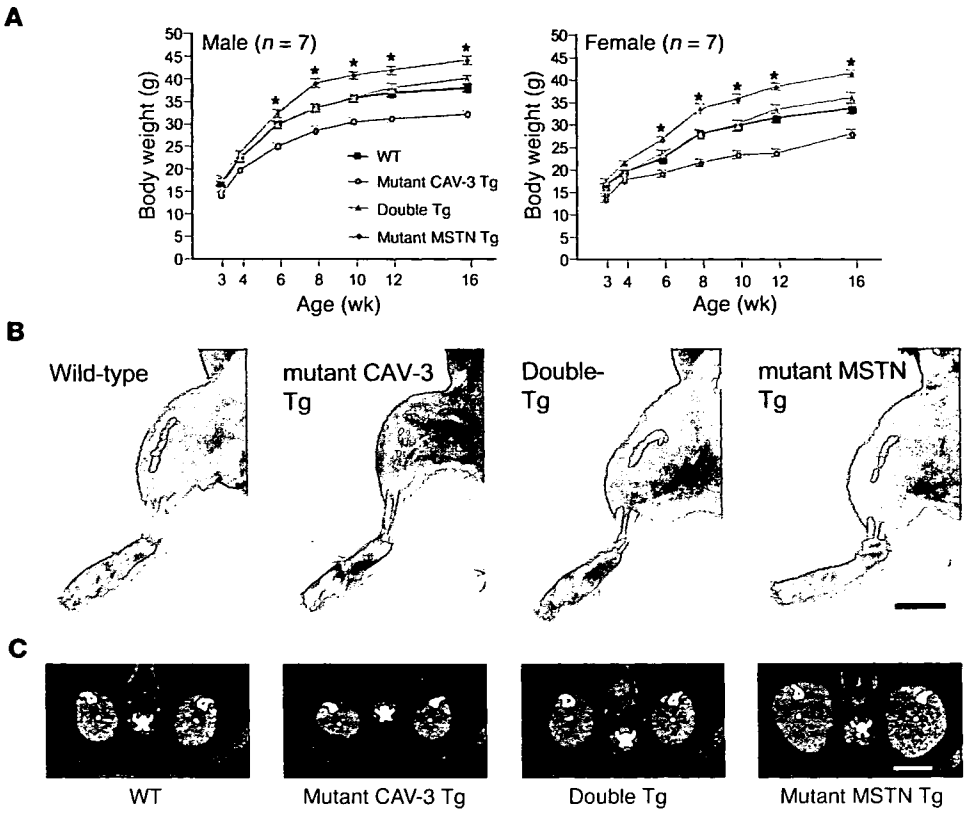

Figure 3
Myostatin inhibition reverses muscular atrophy of mutant caveolin-3–Tg mice. **(A)** Comparison of body weight of mice at 3, 4, 6, 8, 10, 12, and 16 weeks of age. Data are expressed as mean ± SD (n = 7). *P < 0.05. **(B)** Appearance of skinned hind limbs from 10-week-old mice of the 4 distinct genotypes. Scale bar: 5 mm. **(C)** Axial computed tomographic scans of the center of distal hind limbs in 10-week-old mice. Scale bar: 5 mm. Mutant CAV-3 Tg, CAV-3^{P104L}; mutant MSTN Tg, MSTN^{Pro}; double Tg, CAV-3^{P104L}/MSTN^{Pro}.

Caveolin-3 inhibits myostatin-induced transcriptional activity. To determine the effect of caveolin-3 on myostatin-induced transcriptional activity, we performed a transcriptional assay using a Smad-responsive luciferase reporter gene (13, 25). HEK293 human embryonic kidney cells, which do not express endogenous caveolin-3 (Figure 2B), were cotransfected with the luciferase reporter and either empty vector, wild-type caveolin-3, or mutant caveolin-3. Stimulation with recombinant myostatin in HEK293 cells transfected with the empty vector caused a significant increase in luciferase activity above the basal level (Figure 2B). In the wild-type caveolin-3 transformant, myostatin-induced transcriptional activity decreased by approximately 90% (Figure 2B). In contrast, the mutant caveolin-3 transformant showed a 1.5-fold increase in myostatin-induced transcriptional activity. These results indicate that wild-type caveolin-3 functionally inhibits myostatin signaling at the transcriptional level whereas P104L mutant caveolin-3 enhances myostatin signaling.

Introduction of the myostatin prodomain transgene reverses muscular atrophy in the mutant caveolin-3–Tg mice. To determine whether caveolin-3 regulates myostatin signaling in skeletal muscle in vivo and whether myostatin inhibition affects muscular atrophy in caveolin-3–deficient mice, we generated double-Tg mice showing both caveolin-3 deficiency and myostatin inhibition. Heterozygous mating of the mutant caveolin-3–Tg mice (5) with the mutant myostatin–Tg mice (12) gave rise to mice with 4 distinct genotypes: wild-type, mutant caveolin-3–Tg (CAV-3^{P104L}), mutant myostatin–Tg (MSTN^{Pro}), and double Tg (CAV-3^{P104L}/MSTN^{Pro}). The mRNA expression of the transgenes in skeletal muscle was confirmed by Northern blotting (Supplemental Figure 1; supplemental material available online with this article; doi:10.1172/JCI28520DS1). We examined the progressive changes in body weight between 3 and 16 weeks after birth (Figure 3A). The body weights for wild-type, mutant caveolin-3–Tg, and mutant myostatin–Tg were significantly different beginning at 6 weeks and until 16 weeks of age. The mutant caveolin-3–Tg mice were significantly smaller than wild-type mice whereas the double-Tg mice were significantly larger than the mutant caveolin-3–Tg mice and similar in size to the wild-type mice (Supplemental Figure 2). This tendency was found in both sexes. Examination of skinned hind-limb muscle showed that muscular atrophy in the mutant caveolin-3–Tg mice was reversed in the double-Tg mice (Figure 3B). This was also observed in axial computed tomographic scans (Figure 3C). These results suggest that inhibition of myostatin signaling with its prodomain reverses skeletal muscle atrophy in the mutant caveolin-3–Tg mice.

Myostatin inhibition reverses hypoplasia and hypotrophy in mutant caveolin-3–Tg mice. H&E staining and laminin immunostaining of tibialis anterior (TA) muscle showed that reduced myofiber size in the mutant caveolin-3–Tg mice appeared to be reversed in the double-Tg mice even though they were still deficient in caveolin-3 (Figure 4A). To determine whether hypertrophy (i.e., increase of myofiber size) or hyperplasia (i.e., increase of myofiber number) contributed to the restoration of muscle mass in the double-Tg mice, we examined the distribution of single myofiber area and the total myofiber number in the TA muscle (n = 5; Figure 4, B and C). Compared with the wild-type mice, the mutant caveolin-3–Tg mice showed a significant reduction in single myofiber area (1984.7 ± 660.2 versus 844.8 ± 320.2 μm^2; P < 0.05; Figure 4B) and total myofiber number (1663.4 ± 92.2 versus 1125.2 ± 68.6; P < 0.05; Figure 4C). In contrast, the mutant myostatin–Tg mice exhibited a significant increase in single myofiber area (2133.5 ± 632.4 μm^2; P < 0.05 versus wild-type; Figure 4B) and total myofiber number (3336.4 ± 71.3; P < 0.05 versus wild type; Figure 4C). In the double-Tg mice, both

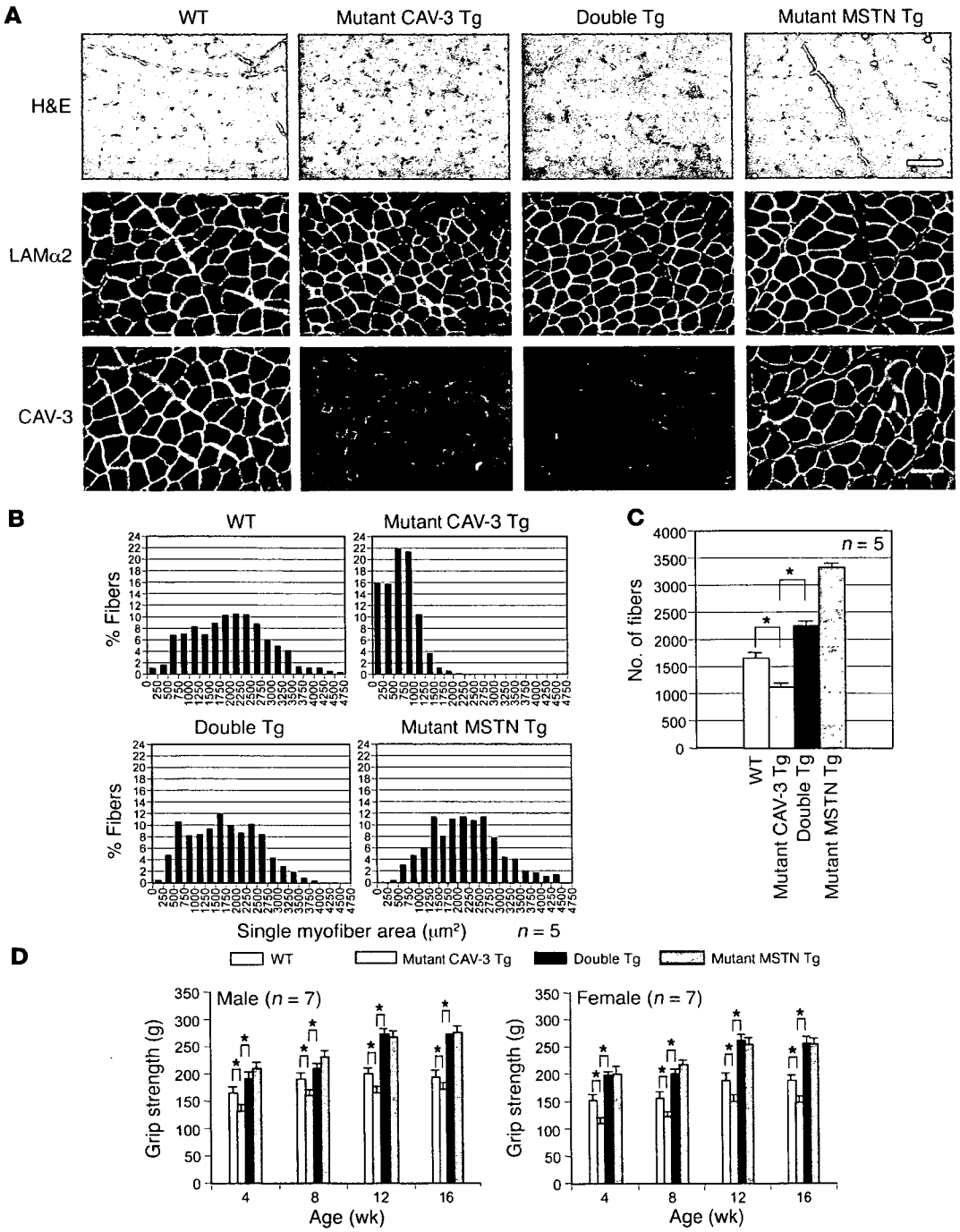

Figure 4
Myostatin inhibition reverses hypoplasia and hypotrophy and enhances muscle strength in mutant caveolin-3–Tg mice. (**A**) Histological and immunohistochemical analyses of TA muscle from 10-week-old mice. LAMα2, laminin α2. Scale bar: 50 μm. (**B**) Distribution of single myofiber area of TA muscle from mice at 10 weeks of age (n = 5; 250 myofibers measured for each mouse). (**C**) Total numbers of myofibers of TA muscle from mice at 10 weeks of age. Data are expressed as mean ± SD (n = 5). *P < 0.05. (**D**) Peak force measurements (g) of grip strength of mice at 4, 8, 12, and 16 weeks of age. Data are expressed as mean ± SD (n = 7). *P < 0.05.

the single myofiber area (1898.6 ± 642.1 μm²; Figure 4B) and the total myofiber number (2252.8 ± 85.5; Figure 4C) were significantly (P < 0.05) increased compared with the mutant caveolin-3–Tg mice. Thus, myostatin inhibition reverses both myofiber hypotrophy and hypoplasia in caveolin-3–deficient skeletal muscle.

Myostatin inhibition reverses muscle weakness in the mutant caveolin-3–Tg mice in vivo. We evaluated skeletal muscle function by measuring the peak force (g) of grip strength between 4 and 16 weeks after birth. The mutant caveolin-3–Tg mice were significantly weaker, and the mutant myostatin-Tg mice were significantly stronger than the wild-type mice at all ages examined (n = 7; Figure 4D). The double-Tg mice were also significantly stronger than the mutant caveolin-3–Tg mice and were as strong as the mutant myostatin-Tg mice (Figure 4D). Furthermore, a treadmill exercise test showed that impaired running ability in the mutant caveolin-3–Tg mice was recovered in the double-Tg mice (Supplemental Figure 3). Muscle weakness in the caveolin-3–deficient mice was rescued by myostatin inhibition.

The amount of prodomain bound to endogenous myostatin is abundant in the mutant myostatin-Tg or the double-Tg mouse skeletal muscle. To examine the possibility that the transgene-derived prodomain binds to C terminal myostatin in vivo, we performed

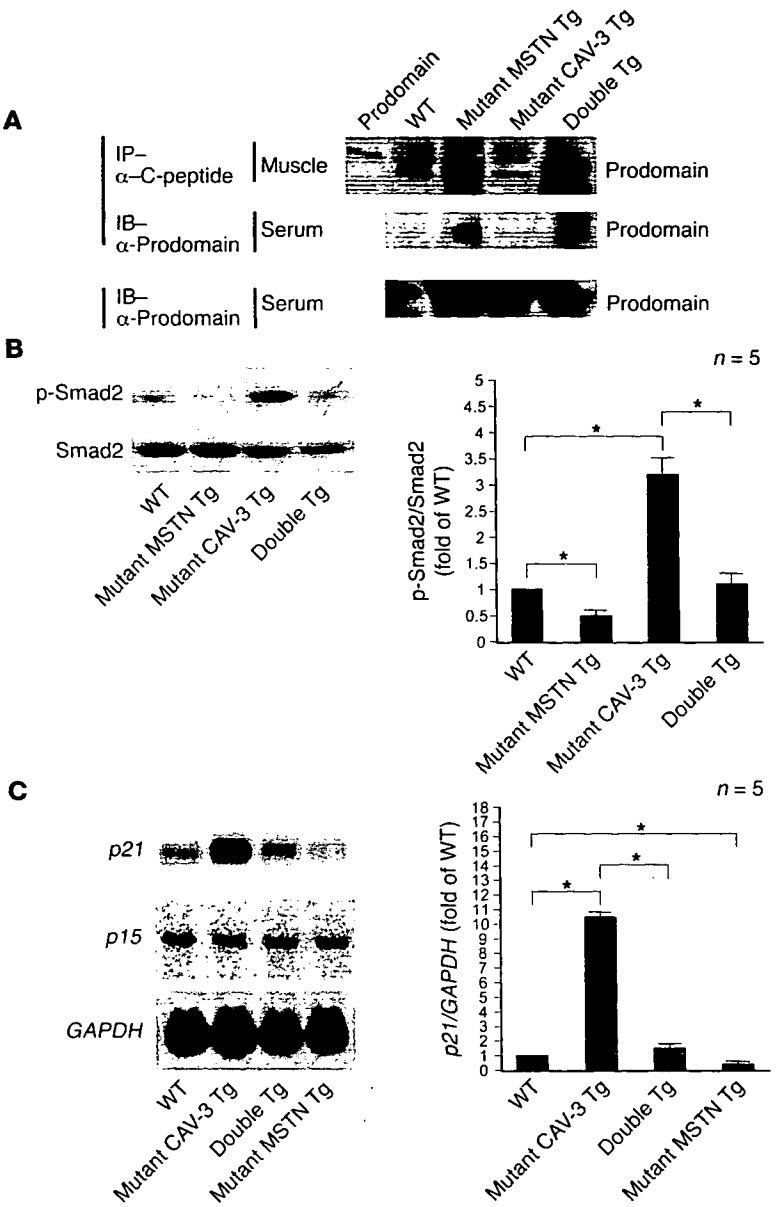

Figure 5

Myostatin inhibition suppresses hyperphosphorylation of Smad2 and increased *p21* expression in caveolin-3–deficient muscle. (**A**) Prodomain C terminal myostatin complex was immunoprecipitated from mouse crude skeletal muscle homogenates (top panel) or sera (middle panel) with an Ab against the myostatin C terminal peptide (α–C-peptide), then immunoblotted (IB) using a polyclonal Ab against the prodomain (α-prodomain). Recombinant myostatin prodomain is used as a control. Immunoblot analysis of sera (bottom panel) shows an excessive amount of prodomain putatively derived from the transgene in the mutant myostatin–Tg mice as well as the double-Tg mice. (**B**) Immunoblot analysis of total Smad2 and p-Smad2 in crude skeletal muscle homogenates from mice (left). Quantification of the p-Smad2/Smad2 ratio by densitometric analysis (right). Values are represented as fold increase with respect to wild-type mice. Data are expressed as mean ± SD ($n = 5$). $^*P < 0.05$. (**C**) Northern blot analysis in mouse skeletal muscle for *p21* and *p15*, which are myostatin-dependent and -independent CDK inhibitors, respectively (left). Quantification of the *p21/GAPDH* ratio by densitometric analysis (right). Values are represented as fold increase with respect to wild-type mice. Data are expressed as mean ± SD ($n = 5$). $^*P < 0.05$.

immunoprecipitation analysis using an Ab against the C terminal myostatin, followed by immunoblotting with an Ab against the prodomain as described previously (26, 27). An excessive amount of prodomain was immunoprecipitated with the endogenous C terminal myostatin from the skeletal muscle and serum in both the mutant myostatin-Tg mice and the double-Tg mice (Figure 5A). The expression level of the prodomain was also very high in both mutant MSTN Tg and double-Tg mice in immunoblot analysis of sera (Figure 5A). These results suggest that transgene-derived prodomain binds to endogenous C terminal myostatin in vivo.

Myostatin inhibition suppresses increased Smad2 phosphorylation in caveolin-3–deficient atrophic muscle. To investigate the status of intracellular myostatin signaling in vivo, we examined the levels of Smad2 and p-Smad2 in crude skeletal muscle homogenates ($n = 5$ per genotype) by immunoblotting and subsequent densitometric analysis (Figure 5B). The amount of total Smad2 protein was unchanged whereas the level of p-Smad2 was significantly reduced in the mutant myostatin-Tg mice. In sharp contrast, there was a significant increase in the levels of p-Smad2 in the mutant caveolin-3–Tg mouse muscle. In the double-Tg mice, the level of p-Smad2 was significantly reduced compared with that in the caveolin-3–Tg mice and was similar to that in the wild-type mice. These results suggest that enhanced myostatin signaling resulting from a loss of caveolin-3 is suppressed by myostatin inhibition in the double-Tg mice.

Myostatin suppresses muscle cell growth via transcriptional regulation of the cyclin-dependent kinase (CDK) inhibitor p21 (22). Therefore we further investigated the expression profile of *p21* in skeletal muscle ($n = 5$ per genotype) by Northern blotting and densitometric analysis (Figure 5C). As expected, the level of *p21* mRNA was significantly reduced in the mutant myostatin-Tg mice. In contrast, the level of *p21* transcripts was significantly increased in mutant caveolin-3–Tg mice. In the double-Tg mice, the level of *p21* expression was significantly reduced compared with that in the caveolin-3–Tg mice and was comparable to that in wild-type mice.

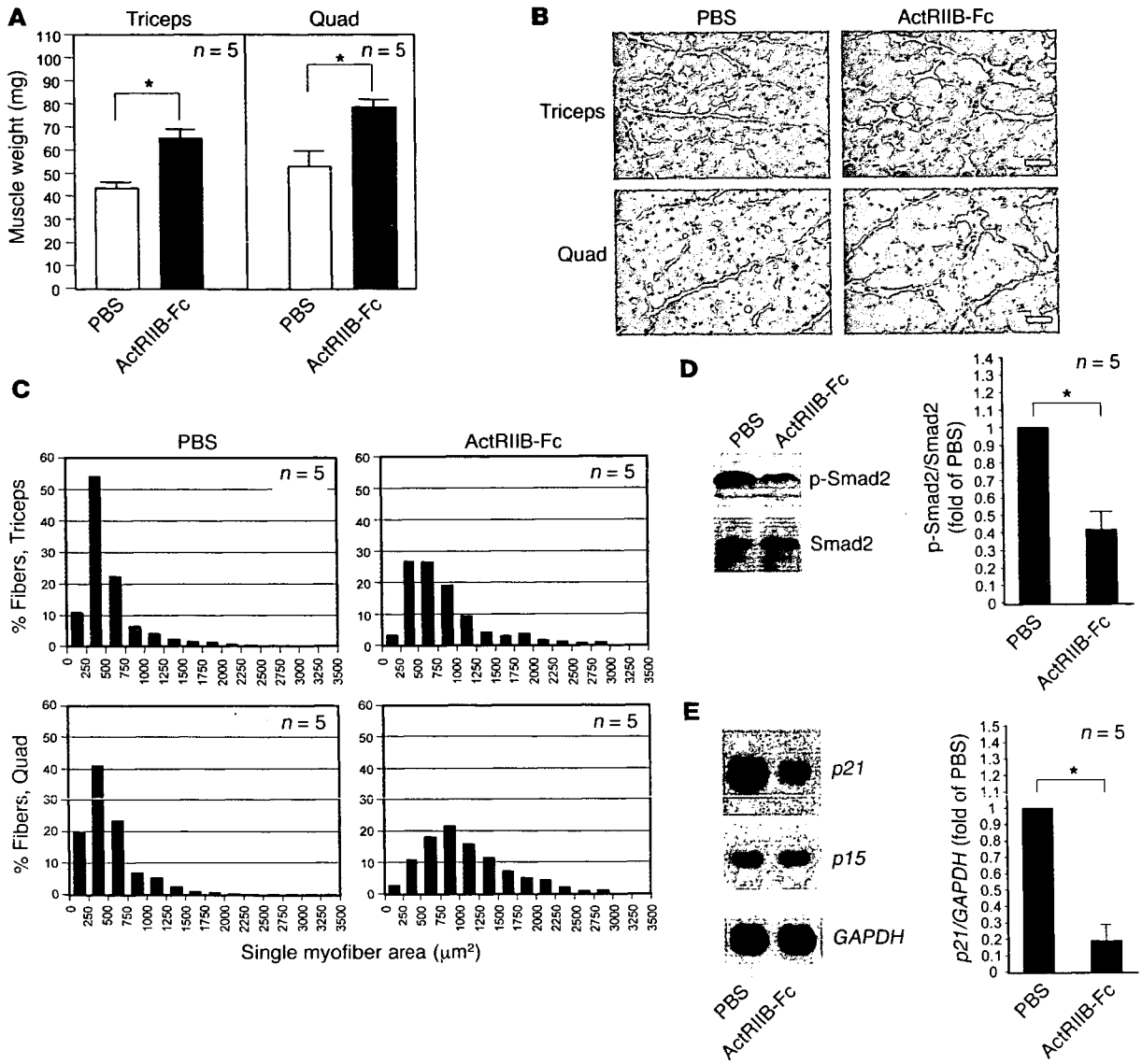

Figure 6

Intraperitoneal injection of the ActRIIB-Fc fusion protein ameliorates muscular atrophy of caveolin-3 deficiency with inhibition of myostatin signaling. (**A**) Comparison of muscle weight (mg) between mutant caveolin-3–Tg mice injected with ActRIIB-Fc and those injected with PBS on day 18. Triceps, triceps brachii muscle; quad, quadriceps femoris muscle. Data are expressed as mean ± SD ($n = 5$). *$P < 0.05$. (**B**) H&E staining of triceps and quadriceps muscles from mice injected with ActRIIB-Fc or PBS. Scale bar: 50 μm. (**C**) Distribution of single myofiber area of triceps and quadriceps muscles on day 18 from mice injected with ActRIIB-Fc or PBS ($n = 5$; 250 myofibers measured for each mouse). (**D**) Immunoblot analysis of total Smad2 and p-Smad2 in crude muscle homogenates from mice injected with ActRIIB-Fc or PBS (left). Quantification of p-Smad2/Smad2 ratio by densitometric analysis (right). Values are represented as fold increase with respect to PBS-injected mice. Data are expressed as mean ± SD ($n = 5$). *$P < 0.05$. (**E**) Northern blot analysis in muscles from mice injected with ActRIIB-Fc or PBS for *p21* and *p15* (left). Quantification of the *p21/GAPDH* ratio by densitometric analysis (right). Values are represented as fold increase with respect to PBS-injected mice. Data are expressed as mean ± SD ($n = 5$). *$P < 0.05$.

Also, there was no change in the mRNA level of *p15*, a myostatin-independent CDK inhibitor (22) (Figure 5C). Increased transcription of *p21* caused by a loss of caveolin-3 was reversed by myostatin inhibition in the double-Tg mice. Thus, these data suggest that myostatin inhibition suppresses enhanced intracellular myostatin signaling in caveolin-3–deficient muscle.

Intraperitoneal injection of the soluble type II myostatin receptor ameliorates muscular atrophy in mutant caveolin-3–Tg mice. To investigate the therapeutic potential of myostatin inhibition for the future treatment of LGMD1C patients, the soluble ActRIIB-Fc fusion protein, which can inhibit myostatin-ActRIIB binding (19, 24), was intraperitoneally injected into the mutant caveolin-3–Tg mice ($n = 5$). Injection of ActRIIB-Fc protein significantly increased the weight of triceps and quadriceps femoris muscles when compared with the control injection of PBS. H&E staining of triceps and quadriceps femoris muscle showed increased myofiber size in the ActRIIB-Fc–injected mice (Figure 6B). Since postnatal growth of skeletal muscle occurs by myofiber hypertrophy

(28), we examined the distribution of single myofiber area in these muscles. Compared with the PBS-injected mice, ActRIIB-Fc-injected mice showed a significant increase in single myofiber area in triceps brachii muscle (507.3 ± 204.1 versus 830.6 ± 304.4 μm^2; $P < 0.05$; $n = 5$) and quadriceps femoris muscle (642.3 ± 234.2 versus 1067.9.4 ± 441.4 μm^2; $P < 0.05$; $n = 5$; Figure 6C). As expected, the levels of p-Smad2 and *p21* transcripts were significantly decreased in the ActRIIB-Fc-injected mice compared with those in the PBS-injected mice (Figure 6, D and E). Thus, postnatal myostatin inhibition also reverses muscular atrophy in the caveolin-3–deficient mice in association with decreased Smad2 phosphorylation and decreased p21 expression.

Discussion

Identification of the molecular mechanism leading to muscular atrophy in the caveolin-3–deficient muscle has remained elusive (4–7). Caveolin-3 plays important roles in muscle cell signal transduction by acting as a scaffolding protein (1–3); however, the signal crosstalk between caveolin-3 and TGF-β superfamily members, including myostatin, has not been previously described. In the present study, we investigated molecular and functional interaction between caveolin-3 and myostatin to better understand the pathogenesis of muscular atrophy in caveolin-3 deficiency and also tested the therapeutic potential of myostatin inhibition for the treatment of caveolin-3 deficiency.

We found that caveolin-3 colocalizes and coimmunoprecipitates with ALK4 or ALK5 type I myostatin receptor in transfected COS-7 cells and that it inhibits activation of ALK4 and ALK5 in vitro. Caveolins bind to and regulate several signaling molecules via the scaffolding domain (2, 3). Caveolin-binding proteins commonly possess specific caveolin-binding motifs (ϕXϕXXXXϕ, ϕXXXXϕXXϕ, and ϕXϕXXXXϕXXϕ, where ϕ indicates an aromatic or aromatic-like amino acid) (3). We examined the amino acid sequences of ALK4 and ALK5 (29) and found that there are putative caveolin-3–binding motifs in the cytoplasmic protein kinase domains of ALK4 (331IAHRDLKSKNILVKK345, 390INMKHFDSFKCADIY404, and 426YQLPYYDLV436) and ALK5 (329IAHRDLKSKNILVKK343, 388INMKFESFKRADIY402, and 424YQLPYYDLV432, where underlines indicate aromatic or aromatic-like amino acids). Thus, the inhibition of the type I myostatin receptor by caveolin-3 may be due to a direct interaction between the caveolin-3 scaffolding domain and caveolin-3–binding motifs in the kinase domain of type I myostatin receptors. Alternatively, caveolin-3 may facilitate raft/caveolae-mediated endocytic degradation of ligand-bound myostatin receptors because the degradation of ligand-bound TGF-β1 receptors is mediated by caveolin-1–coated endocytic vesicles and is accelerated by caveolin-1 (30, 31). Further studies are needed to clarify the mechanism of how caveolin-3 inhibits activation of type I myostatin receptor.

We also demonstrated that wild-type caveolin-3 inhibits downstream intracellular events in myostatin signaling, namely phosphorylation of an effector, Smad2, and transcription of a Smad-responsive reporter gene in vitro. Other groups have demonstrated that the phosphorylation of Smad2 is mediated by activation of ALK4 or ALK5 (20, 21). Taken together, our results indicate that caveolin-3 negatively regulates Smad2 phosphorylation and subsequent transcription by inhibiting activation of type I myostatin receptors. Interestingly, in contrast to wild-type caveolin-3, P104L mutant caveolin-3 enhances autophosphorylation of type I receptor, subsequent Smad2 phosphorylation, and downstream transcriptional activity. Thus, the mutant caveolin-3 molecule could have a toxic gain of function.

We found that both hypoplasia and hypotrophy contribute to skeletal muscle atrophy in the mutant caveolin-3–Tg mice. Previous studies in *mdx* mice, a mouse model of muscular dystrophy caused by dystrophin deficiency, demonstrated that the myofiber number in atrophic muscles was not decreased compared with skeletal muscles from control mice (32, 33). Thus, both muscle hypoplasia and hypotrophy are characteristic of caveolin-3 deficiency. In contrast, the mutant myostatin-Tg mice showed an opposite effect on myofibers (i.e., both hyperplasia and hypertrophy). These opposite effects of caveolin-3 deficiency and myostatin inhibition on myofibers suggested that caveolin-3 interacts with myostatin signaling pathways in muscle cells in vivo.

Therefore, to investigate the in vivo interaction of caveolin-3 and myostatin signaling, we mated P104L mutant caveolin-3–Tg mice with mutant myostatin-Tg mice overexpressing the myostatin prodomain to generate the double-Tg mice with both a caveolin-3 deficiency and myostatin inhibition. We found that myostatin inhibition in the double-Tg mice reversed the skeletal muscle atrophy and weakness observed in the mutant caveolin-3–Tg mice. A morphometric study demonstrated that both hypoplasia and hypotrophy seen in the skeletal muscle of mutant caveolin-3–Tg mice was reversed in the double-Tg mice. After confirming that an excessive amount of prodomain bound to endogenous C terminal myostatin in the mutant myostatin-Tg mice and double-Tg mice in vivo, we further investigated intracellular myostatin signaling in mouse skeletal muscles to clarify the mechanism by which myostatin inhibition rescues muscle atrophy in caveolin-3–deficient mice. Skeletal muscle from mutant myostatin-Tg mice showed a decrease in p-Smad2 protein and downregulation of *p21*, a myostatin-dependent CDK inhibitor (22). These results agree with previous in vitro studies showing that myostatin induces Smad2 phosphorylation and increases *p21* transcription (20–22) and an in vivo study demonstrating that overexpression of myostatin enhances the expression of *p21* in mouse skeletal muscle (9). Notably, we found that skeletal muscle from the mutant caveolin-3–Tg mice increased p-Smad2 protein and upregulated p21, which is consistent with our in vitro results. Importantly, the double-Tg mice showed levels of p-Smad2 and *p21* transcription in the skeletal muscle comparable to those of the wild-type mice, even though they were still deficient in caveolin-3. Consistent with the results from the double-Tg mice, we found that intraperitoneal injection of the soluble type II myostatin receptor ActRIIB-Fc (24) into the mutant caveolin-3–Tg mice also ameliorated muscle atrophy in association with decreased p-Smad2 and *p21*. These in vivo results suggest that overactivation of the intracellular myostatin signal resulting from loss of caveolin-3 plays a significant role in skeletal muscle atrophy in the LGMD1C model mice. In the current study, however, we cannot conclude that hyperphosphorylation of Smad2 and upregulated *p21* expression in caveolin-3–deficient skeletal muscle result simply from overactivation of myostatin signaling, since myostatin prodomain or soluble type II myostatin receptor may suppress not only myostatin but also other TGF-β ligands, including growth and differentiation factor 11 (GDF11) (13, 19, 24, 34, 35). In fact, injection of the soluble type II myostatin receptor further increased skeletal muscle mass of muscular myostatin knockout mice (24). Thus, TGF-β ligands other than myostatin also could be involved in the pathogenesis of muscular atrophy of caveolin-3 deficiency via Smad2-p21–mediated pathway.

Consistent with our results, Sotgia et al. recently reported that mammary epithelial cells derived from caveolin-1 null mice showed constitutively active TGF-β signaling, including epithelial mesenchymal transition and hyperphosphorylation of Smad2 (36). This report, together with their previous results (23) and our current results, indicates that caveolins may suppress TGF-β superfamily–mediated growth inhibition signaling in the isotype- and cell type-specific manner: specifically, these data suggest that caveolin-1 suppresses TGF-β1–mediated signaling in nonmuscle cells while caveolin-3 suppresses myostatin activity in muscle cells. Our current in vitro and in vivo data suggest a novel intracellular regulatory mechanism of myostatin by caveolin-3 that prevents myostatin-induced skeletal muscle atrophy.

Myostatin inhibition therapy has recently been considered for the treatment of muscular dystrophy (37–39). Intraperitoneal administration of a mAb against myostatin or the myostatin prodomain improves the phenotype of *mdx* mice (37, 38); however, the precise molecular mechanism by which myostatin inhibition improves the phenotype of dystrophin-deficient skeletal muscle is not fully understood, and, to our knowledge, an interaction between myostatin and the dystrophin-glycoprotein complex has not been previously reported. Moreover, myostatin inhibition therapy does not improve the phenotype but rather increases the postnatal lethality of *dy* mice, a mouse model of muscular dystrophy with laminin α2 deficiency (39). Therefore, myostatin inhibition therapy does not appear to be effective for all types of muscular dystrophy. It will be necessary to determine to which types of muscular dystrophy myostatin inhibition therapy could be applied and what the rescue mechanism of myostatin inhibition for muscular dystrophy is. Our present data suggest that myostatin inhibition may be a reasonable and promising therapy for caveolin-3–deficient muscular dystrophy associated with enhanced myostatin signaling. Indeed, myostatin inhibition is likely to be more successful in LGMD1C patients than in those with other types of muscular dystrophy.

Methods

Plasmid constructs. Total RNA (1 μg) from mouse or human skeletal muscle was reverse-transcribed with oligo(dT)$_{12-18}$ primer and then subjected to PCR using the following primer sets: caveolin-3, 5′-CGGGATCCATGATGACCGAAGAGCACAC-3′ (*Bam*HI–CAV-3F, forward) and 5′-GGAATTCTTAGCCTTCCCTTCGCAGCAC-3′ (*Eco*RI–CAV-3R, reverse); caveolin-3 with C terminal FLAG-tag, *Bam*HI–CAV-3F and 5′-GGAATTCTTACTTATCATCATCATCCTTGTAGTCGCCTTCCCTTCGCAGCAC-3′ (*Eco*RI–FLAG-CAV-3R, reverse); caveolin-3 with C terminal HA-tag, *Bam*HI–CAV-3F and 5′-GGAATTCTTAGGCGTAATCGGGGACGTCATAAGGGTAGTCGCCTTCCCTTCGCAGCAC-3′ (*Eco*RI–HA–CAV-3R, reverse); ALK4 with C terminal FLAG-tag, 5′-CCGGAATTCATGGCGGAGTCGGCCGGAGCC-3 (*Eco*RI-ALK4F, forward) and 5′-CCGCTCGAGCTACTTATCATCATCATCCTTGTAGTCGATCTTCACGTCTTCCTGCACG-3′ (*Xho*I-FLAG-ALK4R, reverse); and ALK5 with an N terminal FLAG-tag, 5′-CCATCGATATGGAGGCGGCGGTCGCTGCTC-3′ (*Cla*I-ALK5F, forward) and 5′-TGGCTGCAGTTACTTATCATCATCATCCTTGTAGTCCATTTTGATGCCTTCCTGTTG-3′ (*Pst*I-FLAG-ALK5R, reverse). The PCR products were subcloned into the pCS2+ vector (40) using the appropriate restriction sites. Using the QuickChange Site-Directed Mutagenesis Kit (Stratagene), the P104L mutation of caveolin-3 cDNA was introduced into pCS2+wild-type caveolin-3 vector or pCS2+C terminal FLAG-tagged wild-type caveolin-3 vector with the following primers: 5′-CACATCTGGGCCGTGGTGCTCTGCATTAAGAGCTACCTG-3′ (P104L–CAV-3F, forward) and 5′-CAGGTAGCTCTTAATGCAGAGCACCACGGCCCAGATGTG-3′ (P104L–CAV-3R, reverse). HA-tagged ALK4, HA-tagged constitutively active ALK4, HA-tagged ALK5, and HA-tagged constitutively active ALK5 were constructed and provided by K. Miyazono (University of Tokyo, Tokyo, Japan) and T. Imamura (The Cancer Institute of the Japanese Foundation for Cancer Research) as described previously (41, 42). The pGL3-(CAGA)$_{12}$–luciferase reporter containing the Smad-binding sequence (CAGA) was provided by C.-H. Heldin (Uppsala University, Uppsala, Sweden) (24). The pCMV–β-gal vector was used as described previously (43).

Cell culture, transfection, and induction. HEK293 human embryonic kidney and COS-7 monkey kidney cells were maintained in DMEM containing 10% FBS, 2 mM L-glutamine, 0.1 mM nonessential amino acids, and 50 μg/ml kanamycin. Cells were transfected with plasmid DNA–lipid complex using the FuGENE 6 transfection reagent (Roche Diagnostics) according to the manufacturer's protocol. Recombinant myostatin (R&D Systems) was prepared as a 100 μg/ml stock solution in 0.1% BSA with 4 mM HCl.

Immunofluorescence and immunoprecipitation analyses of transfected cells. COS-7 cells cotransfected with FLAG-tagged caveolin-3 and HA-tagged type I receptor were fixed, permeabilized, and double-stained with anti-rabbit caveolin-3 polyclonal Ab (BD Bioscience) and an anti-HA mAb 12CA5 (Roche Diagnostics) for 60 minutes. After washing with PBS, the cells were incubated for 30 minutes with Alexa Fluor 488–conjugated anti-rabbit and Alexa Fluor 594-conjugated anti-mouse IgG Abs (Invitrogen). Immunofluorescent images were captured using a TCS SP2 Laser Scanning Confocal Microscope (Leica Microsystems). For immunoprecipitation, COS-7 cells cotransfected with FLAG- or HA-tagged caveolin-3 and HA- or FLAG-tagged type I receptor were incubated for 30 minutes on ice with a lysis buffer containing 50 mM Tris-HCl (pH 7.4), 50 mM NaCl, 1% Triton X-100, and 100 mM octyl glucoside (Sigma-Aldrich) supplemented with a proteinase inhibitor cocktail (complete, EDTA-free; Roche Diagnostics). Cells were precleared by centrifugation at 10,000 *g* for 30 minutes, after which anti-FLAG mAb M2 agarose gel (Sigma-Aldrich) was added to precleared lysates. After rotary mixing for 2 hours at 4°C, immunoprecipitates were washed 3 times with lysis buffer. The immunoprecipitates or whole cell lysates were separated by SDS-PAGE (3% to 18% linear gradient of acrylamide), transferred to a PVDF membrane, and subjected to immunoblot analysis. The membrane was blocked with 5% milk in Tris-buffed saline (50 mM Tris-HCl [pH 7.5] and 137 mM NaCl) containing 0.1% Tween-20 and then incubated overnight at 4°C with anti-FLAG mAb M2 (Sigma-Aldrich) or anti-HA mAb 12CA5. After washing with Tris-buffered saline containing 0.1% Tween-20, the blots were incubated with horseradish-conjugated anti-mouse IgG Ab (Amersham Biosciences). Immunoreactive bands were visualized using ECL reagents (Amersham Biosciences).

In vitro autophosphorylation of constitutively active ALK4 or ALK5. Lysates from COS-7 cells cotransfected with FLAG-tagged wild-type or P104L mutant caveolin-3 and HA-tagged constitutively active forms of type I receptor, ALK4 or ALK5, were immunoprecipitated with anti-HA 12CA5 agarose gel (Sigma-Aldrich). Immunoprecipitates of constitutively active ALK4 or ALK5 were equilibrated with 50 μl of kinase reaction buffer (40 mM HEPES [pH 7.4], 10 mM $MgCl_2$, 3 mM $MnCl_2$, 10 mM β-glycerol-phosphate, 10 mM NaF, and 2 mM DTT) for 5 minutes on ice. The kinase reaction was initiated by adding 10 μCi of [γ-^{32}P]ATP. After incubation for 20 minutes at 25°C, the reaction was terminated by addition of 50 μl of ×2 SDS-PAGE sample buffer and boiling for 5 minutes. The sample was subsequently subjected to SDS-PAGE (3% to 18% linear gradient of acrylamide), and phosphorylated constitutively active ALK4 or ALK5 was detected by autoradiography using a Fuji Imaging Plate (Fujifilm). Total type I receptor or caveolin-3 was immunoblotted using anti-HA mAb 12CA5 or anti-FLAG mAb M2.

In vitro analysis of Smad2 phosphorylation. Recombinant myostatin was added to COS-7 cells transfected with wild-type caveolin-3, P104L mutant caveolin-3, or empty vector control. After 24 hours, cells were lysed in PBS

containing 1 mM EDTA and 0.1% Triton X-100, and resulting cell lysates were subjected to immunoblot analysis using a rabbit polyclonal Ab against Smad2 or p-Smad2 (Ser465/467; Cell Signaling Technology).

Luciferase assays for myostatin activity. HEK293 cells were seeded in 12-well plates at a density of 1.0×10^5 cells per well and cultured for 24 hours. Cells were then cotransfected with the pGL3-$(CAGA)_{12}$-luciferase reporter gene, the pCMV-β-gal, and either empty vector (pCS2+), wild-type caveolin-3 (pCS2 + wild-type CAV-3), or P104L mutant caveolin-3 (pCS2 + mutant CAV-3). After 24 hours, medium was replaced with serum-free DMEM containing 20 ng/ml recombinant myostatin. After an additional 24 hours, cells were lysed with ×1 lysis buffer (Promega), and luciferase activity in the cell lysates was determined by a luciferase reporter assay system (Promega) using an LB9506 MiniLumat Luminometer (Berthold Technologies). Luciferase activities were normalized by β-gal activity as described previously (43).

Generation of double-Tg mice coexpressing P104L mutant caveolin-3 and myostatin prodomain. We previously generated CAV-3^{P104L} and $MSTN^{Pro}$ mice (5, 12). Heterozygous mating of these mice gave rise to F1 offspring with 4 distinct genotypes: wild-type, mutant caveolin-3–Tg (CAV-3^{P104L}), mutant myostatin-Tg ($MSTN^{Pro}$), and double Tg (CAV-3^{P104L}/$MSTN^{Pro}$). The presence of transgenes (P104L caveolin-3 or myostatin prodomain) was determined by PCR amplification from tail DNA as described previously (5, 12). All animal experiments were performed at the Laboratory Animal Center with the approval of the Animal Research Committee at the Kawasaki Medical School.

Computed tomographic analysis of muscle volume. Axial-computed tomography at the center of the distal hind limb in mice was performed using a LaTheta LTC-100 (Aloka).

Immunohistochemical and morphometric analyses. Unfixed distal hind limbs of mice were snap-frozen in liquid nitrogen–cooled isopentane and sectioned transversely (10 μm) at the center of the TA muscle using a cryostat (Leica Microsystems) with an A35 Microtome Blade (Tech-Jam) as described previously (44). Sections were postfixed in 1% formalin in PBS for 10 minutes and then immunostained according to the M.O.M. procedure (Vector Mouse on Mouse Kit; Vector Laboratories) using a rabbit polyclonal Ab against caveolin-3 (BD Biosciences) or a rat mAb against laminin α2 (clone 4H8-2; Sigma-Aldrich) followed by rabbit or rat FITC-conjugated secondary Abs. The single myofiber area in the TA muscle ($n = 5$; 250 myofibers measured for each mouse) and the total myofiber number in the TA muscle ($n = 5$) were measured from the fluorescence images of anti-laminin α2-stained sections using the 2-color technique with Lumina Vision software version 2.0 (Mitani Corp.).

Grip strength and treadmill exercise tests. Mice grasping wire mesh with their forelimbs and hind limbs were pulled horizontally by their tails until they lost their grip. Peak grip strength (g) was measured using an MK-380S automated Grip Strength Meter (Muromachi). For Supplemental Video 1, the mice were placed on an MK-680S treadmill (Muromachi) with a shock bar (1 mA) and run at 14 m/min for 10 minutes.

Immunoprecipitation and immunoblot analyses of skeletal muscles and sera. As described previously (26, 27), myostatin was immunoprecipitated from skeletal muscle or serum samples from each mouse at 10 weeks of age using an Ab against the myostatin C terminal peptide (R&D Systems). Immunoblot analysis was performed using a polyclonal Ab against the myostatin prodomain (gift of Wyeth). Control recombinant myostatin prodomain was purchased from R&D Systems. For immunoblot analysis of Smad2 and p-Smad2, skeletal muscle from 10-week-old mice was homogenized in 10 volumes (w/v) of a buffer consisting of 50 mM Tris-HCl (pH 7.4), 100 mM NaCl, 1 mM EDTA, 5 mM β-mercaptoethanol, 0.1 mM PMSF, and 1 mM benzamidine. The crude extracts were separated by SDS-PAGE (3% to 18% linear gradient of acrylamide) and transferred to PVDF. Immunoblot analysis was performed using the same Abs described for in vitro analysis of Smad2 phosphorylation.

Northern blot analysis. RT-PCR products of mutant caveolin-3 transgene (5), mutant myostatin transgene (12), mouse p21 (nt1-255), and mouse p15 (nt1-421) were subcloned into the pCRII-TOPO vector (Invitrogen) and then digested with *Eco*RI. The digested insert was separated by agarose gel electrophoresis and extracted using a Rapid Gel Extraction System (Marligen Bioscience). Each DNA fragment was then labeled with [α-^{32}P]dCTP using the MegaPrime DNA Labeling System (Amersham Biosciences). Twenty micrograms of total RNA from the skeletal muscle of a 10-week-old mouse from each strain was separated on a 0.7% agarose gel containing 7% formaldehyde and blotted onto Hybond-N+ (Amersham Biosciences). Hybridization was performed at 42°C for 24 hours, and autoradiography was performed using a Fuji Imaging Plate (Fujifilm).

Intraperitoneal injection of the ActRIIB-Fc fusion protein to mutant caveolin-3–Tg mice. According to the method described previously (24), 10 mg/kg of human ActRIIB-Fc fusion protein, purchased from R&D Systems, was injected into 6-week-old P104L mutant caveolin-3–Tg mice on days 1, 4, 8, and 15 ($n = 5$). Mice were sacrificed on day 18 for analysis of skeletal muscle. Morphometrical analysis of single myofiber area in the triceps brachii and quadriceps femoris muscles ($n = 5$; 250 myofibers measured for each muscle), Smad2 phosphorylation analysis, and p21 expression analysis were performed using the same method as described above.

Statistics. Statistical analysis was performed on paired observations using Bonferroni's test after 1-way ANOVA. *P* values less than 0.05 were considered significant.

Acknowledgments

We wish to thank Wyeth and C.-H. Heldin (Uppsala University), K. Miyazono (Department of Molecular Pathology, University of Tokyo), and T. Imamura (Department of Biochemistry, The Cancer Institute of the Japanese Foundation for Cancer Research) for reagents and A.C. McPherron (National Institute of Diabetes and Digestive and Kidney Diseases, NIH) for comments on the manuscript. We are grateful to N. Akazawa for critical reading of the manuscript. We also thank T. Murakami (Division for Therapies against Intractable Diseases, Institute for Comprehensive Medical Science, Fujita Health University), S.-i. Nishimatsu, and T. Nohno (Department of Molecular Biology, Kawasaki Medical School) as well as S. Hirano, H. Kitao, and M. Takata (Department of Immunology, Kawasaki Medical School) for valuable advice, and we thank M. Kita (Laboratory Animal Center, Kawasaki Medical School), K. Yamane, K. Uehira (Electron Microscopy Center, Kawasaki Medical School), N. Naoe, T. Kawase, and Y. Kuroda (Division of Neurology, Kawasaki Medical School) for technical assistance. This work was supported by a research grant for Nervous and Mental Disorders from the Ministry of Health, Labor and Welfare (14B-4); grants for research on Psychiatric and Neurological Diseases and Mental Health from the Ministry of Health, Labor and Welfare of Japan (15131301 and 17231401) and from the Japan Society for the Promotion of Science (KAKENHI 14370212); and by research project grants from Kawasaki Medical School (15-115B, 16-601, and 17-605S).

Received for publication March 14, 2006, and accepted in revised form July 11, 2006.

Address correspondence to: Yoshihide Sunada, Division of Neurology, Department of Internal Medicine, Kawasaki Medical School, 577 Matsushima, Kurashiki, Okayama 701-0192, Japan. Phone: 81-86-462-1111; Fax: 81-86-462-1199; E-mail: ysunada@med.kawasaki-m.ac.jp.

1. Parton, R.G. 2003. Caveolae-from ultrastructure to molecular mechanisms. *Nat. Rev. Mol. Cell Biol.* **4**:162-167.
2. Galbiati, F., Razani, B., and Lisanti, M.P. 2001. Emerging themes in lipid rafts and caveolae. *Cell.* **106**:403-411.
3. Couet, J., Li, S., Okamoto, T., Ikezu, T., and Lisanti, M.P. 1997. Identification of peptide and protein ligands for the caveolin-scaffolding domain. Implications for the interaction of caveolin with caveolae-associated proteins. *J. Biol. Chem.* **272**:6525-6533.
4. Minetti, C., et al. 1998. Mutations in the caveolin-3 gene cause autosomal dominant limb-girdle muscular dystrophy. *Nat. Genet.* **18**:365-368.
5. Sunada, Y., et al. 2001. Transgenic mice expressing mutant caveolin-3 show severe myopathy associated with increased nNOS activity. *Hum. Mol. Genet.* **10**:173-178.
6. Smythe, G.M., Eby, J.C., Disatnik, M.H., and Rando, T.M. 2003. A caveolin-3 mutant that causes limb girdle muscular dystrophy type 1C disrupts Src localization and activity and induces apoptosis in skeletal myocytes. *J. Cell Sci.* **116**:4739-4749.
7. Hernandez-Deviez, D.J., et al. 2006. Aberrant dysferlin trafficking in cells lacking caveolin or expressing dystrophy mutants of caveolin-3. *Hum. Mol. Genet.* **15**:129-142.
8. McPherron, A.C., Lawler, A.M., and Lee, S.-J. 1997. Regulation of skeletal muscle mass in mice by a new TGF-beta superfamily member. *Nature.* **387**:83-90.
9. Zimmers, T.A., et al. 2002. Induction of cachexia in mice by systemically administered myostatin. *Science.* **296**:1486-1488.
10. Reisz-Porszasz, S., et al. 2003. Lower skeletal muscle mass in male transgenic mice with muscle-specific overexpression of myostatin. *Am. J. Physiol. Endocrinol. Metab.* **285**:E876-E888.
11. Grobet, L., et al. 2003. Modulating skeletal muscle mass by postnatal, muscle-specific inactivation of the myostatin gene. *Genesis.* **35**:227-238.
12. Nishi, M., et al. 2002. A missense mutant myostatin causes hyperplasia without hypertrophy in the mouse muscle. *Biochem. Biophys. Res. Commun.* **293**:247-251.
13. Thies, R.S., et al. 2001. GDF-8 propeptide binds to GDF-8 and antagonizes biological activity by inhibiting GDF-8 receptor binding. *Growth Factors.* **18**:251-259.
14. Wolfman, N.M., et al. 2003. Activation of latent myostatin by the BMP-1/tolloid family of metalloproteinases. *Proc. Natl. Acad. Sci. U. S. A.* **100**:15842-15846.
15. Yang, J., et al. 2001. Expression of myostatin pro domain results in muscular transgenic mice. *Mol. Reprod. Dev.* **60**:351-361.
16. Pirottin, D., et al. 2005. Transgenic engineering of male-specific muscular hypertrophy. *Proc. Natl. Acad. Sci. U. S. A.* **102**:6413-6418.
17. Yang, J., and Zhao, B. 2006. Postnatal expression of myostatin propeptide cDNA maintained high muscle growth and normal adipose tissue mass in transgenic mice fed a high-fat diet. *Mol. Reprod. Dev.* **73**:462-469.
18. Massague, J. 1998. TGF-beta signal transduction. *Annu. Rev. Biochem.* **67**:753-791.
19. Lee, S.-J., and McPherron, A.C. 2001. Regulation of myostatin activity and muscle growth. *Proc. Natl. Acad. Sci. U. S. A.* **98**:9306-9311.
20. Rebbapragada, A., Benchabane, H., Wrana, J.L., Celeste, A.J., and Attisano, L. 2003. Myostatin signals through a transforming growth factor beta-like signaling pathway to block adipogenesis. *Mol. Cell. Biol.* **23**:7230-7242.
21. Rios, R., Fernandez-Nocelos, S., Carneiro, I., Arce, V.M., and Devesa, J. 2004. Differential response to exogenous and endogenous myostatin in myoblasts suggests that myostatin acts as an autocrine factor in vivo. *Endocrinology.* **145**:2795-2803.
22. Thomas, M., et al. 2000. Myostatin, a negative regulator of muscle growth, functions by inhibiting myoblast proliferation. *J. Biol. Chem.* **275**:40235-40243.
23. Razani, B., et al. 2001. Caveolin-1 regulates transforming growth factor (TGF)-beta/SMAD signaling through an interaction with the TGF-beta type I receptor. *J. Biol. Chem.* **276**:6727-6738.
24. Lee, S.-J., et al. 2005. Regulation of muscle growth by multiple ligands signaling through activin type II receptors. *Proc. Natl. Acad. Sci. U. S. A.* **102**:18117-18122.
25. Jonk, L.J., Itoh, S., Heldin, C.-H., ten Dijke, P., and Kruijer, W. 1998. Identification and functional characterization of a Smad binding elements (SBE) in the JunB promoter that acts as a transforming growth factor-beta, activin, and bone morphogenetic protein-inducible enhancer. *J. Biol. Chem.* **273**:21145-21152.
26. Hill, J.J., et al. 2002. The myostatin propeptide and the follistatin-related gene are inhibitory binding proteins of myostatin in normal serum. *J. Biol. Chem.* **277**:40735-40741.
27. Schuelke, M., et al. 2004. Myostatin mutation associated with gross muscle hypertrophy in a child. *N. Engl. J. Med.* **350**:2682-2688.
28. Campion, D.R. 1984. The muscle satellite cell: a review. *Int. Rev. Cytol.* **87**:225-251.
29. Feng, X.-H., and Derynck, R.A. 1997. A kinase subdomain of transforming growth factor-beta (TGF-beta) type I receptor determines the TGF-beta intracellular signaling specificity. *EMBO J.* **16**:3912-3923.
30. Di Guglielmo, G.M., Le Roy, C., Goodfellow, A.F., and Wrana, J.L. 2003. Distinct endocytic pathways regulate TGF-beta receptor signalling and turnover. *Nat. Cell Biol.* **5**:410-421.
31. Le Roy, C., and Wrana, J.L. 2005. Clathrin- and non-clathrin-mediated endocytic regulation of cell signalling. *Nat. Rev. Mol. Cell Biol.* **6**:112-126.
32. DiMario, J.X., Uzman, A., and Strohman, R.C. 1991. Fiber regeneration is not persistent in dystrophic (MDX) mouse skeletal muscle. *Dev. Biol.* **148**:314-321.
33. Pastoret, C., and Sebille, A. 1993. Further aspects of muscular dystrophy in mdx mice. *Neuromuscul. Disord.* **3**:471-475.
34. Oh, S.P., et al. 2002. Activin type IIA and IIB receptors mediate Gdf11 signaling in axial vertebral patterning. *Genes Dev.* **16**:2749-2754.
35. De Caestecker, M. 2004. The transforming growth factor-beta superfamily of receptors. *Cytokine Growth Factor Rev.* **15**:1-11.
36. Sotgia, F., et al. 2006. Caveolin-1 deficiency (-/-) conveys premalignant alterations in mammary epithelia, with abnormal lumen formation, growth factor independence, and cell invasiveness. *Am. J. Pathol.* **168**:292-309.
37. Bogdanovich, S., et al. 2002. Functional improvement of dystrophic muscle by myostatin blockade. *Nature.* **420**:418-421.
38. Bogdanovich, S., Perkins, K.J., Krag, T.O.B., Whittemore, L.-A., and Khurana, T.S. 2005. Myostatin propeptide-mediated amelioration of dystrophic pathology. *FASEB J.* **19**:543-549.
39. Li, Z.F., Shelton, G.D., and Engvall, E. 2005. Elimination of myostatin does not combat muscular dystrophy in dy mice but increase postnatal lethality. *Am. J. Pathol.* **166**:491-495.
40. Narita, T., et al. 2005. Wnt10a is involved in AER formation during chick limb development. *Dev. Dyn.* **233**:282-287.
41. Kawabata, M., Inoue, H., Hanyu, A., Imamura, T., and Miyazono, K. 1998. Smad proteins exist as monomers in vivo and undergo homo- and hetero-oligomerization upon activation by serine/threonine kinase receptors. *EMBO J.* **17**:4056-4065.
42. Murakami, G., Watabe, T., Takaoka, K., Miyazono, K., and Imamura, T. 2003. Cooperative inhibition of bone morphogenetic protein signaling by Smurf1 and inhibitory Smads. *Mol. Biol. Cell.* **14**:2809-2817.
43. Funaba, M., et al. 2003. Transcriptional activation of mouse mast cell Protease-7 by activin and transforming growth factor-beta is inhibited by microphthalmia-associated transcription factor. *J. Biol. Chem.* **278**:52032-52041.
44. Sasaoka, T., et al. 2003. Pathological analysis of muscle hypertrophy and degeneration in muscular dystrophy in gamma-sarcoglycan-deficient mice. *Neuromuscul. Disord.* **13**:193-206.

Inhibitors of the TGF-β Superfamily and their Clinical Applications

K. Tsuchida[1,*], Y. Sunada[2], S. Noji[3], T. Murakami[1], A. Uezumi[1] and M. Nakatani[1]

[1]*Division for Therapies against Intractable Diseases, Institute for Comprehensive Medical Science (ICMS), Fujita Health University, Toyoake, Aichi 470-1192, Japan;* [2]*Division of Neurology, Department of Internal Medicine, Kawasaki Medical School, 577 Matsushima, Kurashiki-City, Okayama 701-0192, Japan;* [3]*Department of Biological Science and Technology, Faculty of Engineering, The University of Tokushima, 2-1 Minami-Jyosanjima-cho, Tokushima 770-8506, Japan*

Abstract: The transforming growth factor-β (TGF-β) superfamily includes TGF-βs, activin, myostatin and bone morphogenetic proteins. Misregulation of the activity of TGF-β family members is involved in pathogenesis of cancer, muscular dystrophy, obesity and bone and tooth remodeling. Natural inhibitors for the TGF-β superfamily regulate fine-tuning of activity of TGF-β family *in vivo*. In addition to natural inhibitors for the TGF-β family, soluble forms of receptors for the TGF-β family, blocking monoclonal antibodies and small chemical TGF-β inhibitors have been developed. In this review, we summarize recent advances in our understanding of inhibitors for the TGF-β superfamily and their medical applications.

Key Words: TGF-β, activin, BMP, cancer, fibrosis, follistatin, myostatin, muscular dystrophy.

INTRODUCTION

The transforming growth factor-β (TGF-β) superfamily includes TGF-βs, activin, myostatin and bone morphogenetic proteins (BMPs) [1]. They are involved in many biological responses including growth and differentiation of various cell types. Misregulation of specific TGF-β family members is involved in pathogenesis of certain types of cancer, fibrosis, diseases affecting skeletal muscle, and osteoporosis [2]. Thus, proteins and chemicals that regulate TGF-β family members could be used as drugs for treatment of human diseases.

Members of the TGF-β superfamily bind to type I and type II serine/threonine kinase receptors and transduce intracellular signaling through Smad proteins. TGF-β/activin/myostatin activate Smad2/3, whereas the BMP subfamily activates Smad1/5/8. These pathway-restricted Smads associate with Co-Smad, Smad4 and translocate into the nucleus, and regulate transcription of target genes. Smad6/7 are inhibitory Smads that serve as negative regulators of signaling of the TGF-β family [1]. Signaling of the TGF-β family is regulated by extracellular ligand-binding proteins. Follistatin and related molecules regulate activin/myostatin [2]. Noggin, chordin, Cerberus and differential screening-selected gene aberrative in neuroblastoma (DAN) families are regulators of BMP family members.

Furthermore, TGF-β receptors are dynamically regulated by trafficking of receptors by clathrin-mediated endocytosis and the lipid raft-caveolar pathway [1].

As mentioned above, natural binding proteins for the TGF-β superfamily exist and play an important role in negative regulation of TGF-β signaling. In addition, soluble forms of receptors for the TGF-β superfamily, blocking monoclonal antibodies, and small molecule receptor kinase inhibitors have recently been developed.

Since TGF-β signaling is involved in pathogenesis and progression of various diseases, TGF-β inhibitors are promising as novel drugs for the treatment of cancer, muscular dystrophy, osteoporosis and fibrosis. Myostatin inhibitors such as monoclonal myostatin antibodies, follistatin and myostatin propeptide could be promising lead compounds in drug development for muscular dystrophy. BMP signaling is involved in osteogenesis and tooth development. Therefore, BMP inhibitors could be applicable for osteoporosis and tooth regeneration.

In this mini-review, we summarize recent advances in our understanding of TGF-β inhibitors and their potential medical applications.

OUTLINE OF THE TGF-β SUPERFAMILY

TGF-β family members are pleiotropic cell signaling proteins that play essential roles in tissue homeostasis and development [1]. One of the most salient characteristics of TGF-β family members is inhibition of growth of various cell types. TGF-β is involved in inhibition of cancer cell growth. TGF-β induces cell cycle arrest through upregulation of cyclin-dependent kinase (CDK) inhibitors p21, p27 and p15, resulting in the inhibition of entry through the G1-phase into the S-phase [1,3]. This property of TGF-β has gained much attention for its role in tumor suppression in tumorigenesis. In the later phase of cancer progression, tumor cells become resistant to growth inhibition by TGF-β, and cancer cells secrete TGF-β. TGF-β secreted by cancer stimulates the neighboring epithelial cells and promotes cancer progression through epithelial–mesenchymal transdifferentiation, and promotes metastasis of malignant cells through mediating changes in cytoskeletal architecture [1,4]. Therefore, TGF-β signaling offers an attractive target for cancer therapy. TGF-βs signal through their own type II receptor

*Address correspondence to this author at the Division for Therapies against Intractable Diseases, Institute for Comprehensive Medical Science (ICMS), Fujita Health University, Toyoake, Aichi 470-1192, Japan; Tel: +81-562-93-9384; Fax: +81-562-93-5791; E-mail: tsuchida@fujita-hu.ac.jp

1389-5575/06 $50.00+.00

(TβRII) and type I receptor (activin receptor-like kinase 5 (ALK5)), that are distinct from the type II and type I receptors which activins or BMPs utilize. Several strategies such as the use of antisense oligonucleotides for TGF-β, monoclonal TGF-β antibodies, dominant negative TβRII, and small drug molecules that inhibit TGF-β receptor I kinase have shown great promise in preclinical studies [4].

Activins are homo- or hetero-dimers composed of two β subunits and belong to the TGF-β superfamily. Follistatins are high affinity activin-binding proteins and efficiently neutralize activin functions [2,5]. Activin, inhibin and follistatin are well-recognized as endocrine hormones regulating gonadal functions [2]. However, recent investigation reveals that alteration of activin signaling, like TGF-β, is directly involved in tumor progression. Activins signal through heteromeric complexes of activin type II receptors (ActRIIA and ActRIIB) and type I receptor (ALK4). Two 8-bp polyadenine [(A)8] tracts of the ActRIIA gene were identified as targets for frameshift mutations in gastrointestinal cancers [6]. ALK4 (ACVR1B) gene mutations have also been found in pancreatic carcinoma [7]. Human genes for Smad2 and Smad4 (Dpc4), which act as downstream effectors of activins, TGF-β and myostatin, map to chromosome 18q and are mutated in colorectal and pancreatic carcinomas [8,9]. These findings indicate that alteration of the activin signaling pathway is involved in tumorigenesis.

Cripto, which is the founding member of the epidermal growth factor-Cripto, FRL-1, and Cryptic (EGF-CFC) family, has a role as a co-receptor for nodal [10]. In addition, Cripto binds directly to activin B and inhibits activin B signaling in breast cancer [10]. Blocking Cripto function by a monoclonal antibody suppresses tumor cell growth *in vivo*, most probably through augmentation of activin B signaling by sequestering Cripto from activin B [10]. Taken together, these findings indicate that, as with TGF-β, activins are important regulators of carcinogenesis and have dual roles as tumor suppressors and tumor promoters [11,12].

Myostatin is a recently discovered member of the TGF-β superfamily [13]. Mice lacking the myostatin gene have an ~30 % increase in skeletal muscle mass [13]. Both hyperplasia and hypertrophy are observed in the muscle fibers of myostatin-deficient mice [13]. Myostatin regulates skeletal muscle mass not only in mice but also in cattle and humans. Spontaneous mutations of the myostatin gene have been found in double muscled cattle, called Belgian blue and Piedmontese [14]. Recently, there was a report of a boy who had a splice site mutation in the myostatin gene and who displayed muscle hypertrophy [15]. Blockage of myostatin function, even in adult mice, by a myostatin antibody or conditional gene knockout technology results in an increase in skeletal muscle [16,17]. Thus, inhibition of myostatin is a promising therapeutic approach restoring muscle mass and strength in muscle wasting conditions, such as muscular dystrophy and aging [18].

BINDING PROTEINS FOR THE TGF-β SUPERFAMILY

Activities of the TGF-β superfamily are regulated by their extracellular binding proteins. Several binding proteins such as type III TGF-β receptor facilitate ligand-binding to receptors [19]. However, the majority of TGF-β family binding proteins in the extracellular space sequester ligands to block ligand-binding to receptor serine kinase on the target cells. Research on the mechanism of extracellular regulation of TGF-β signaling by binding proteins provides clues for the treatment of diseases caused by misregulation of the TGF-β signaling pathway [20,21].

Follistatins are best characterized as activin-binding proteins [5,20,22]. Follistatin is a single-chain protein with a molecular mass of 31–39 kDa. Alternative splicing of a single gene and partial proteolysis produces multiple forms of follistatins. All forms of follistatins have an N-terminal domain and three cysteine-rich domains, called follistatin domains, and demonstrate high affinity binding to activins with estimated Kd values of 500–800 pM. Recently, the structures of the follistatin–activin complex were reported [23] (Fig. (**1**)). Two follistatin molecules encircle activin A, neutralizing the ligand by burying one-third of its residues and receptor binding sites. Both type I and II receptor binding sites of activin are blocked by follistatin binding to activin (Fig. (**1**)). Gene knockout studies have revealed that follistatin-deficient mice show numerous phenotypes including musculoskeletal and cutaneous abnormalities [24]. In particular, follistatin-deficient mice show a reduction in the muscle mass of the diaphragm and intercostal muscles. In addition, rib defects and a decreased number of lumbar vertebrae are observed in follistatin gene knockout mice. This finding suggests that follistatin serves as an inhibitor not only for activins but also for other growth and differentiation factor (GDF)/BMP subfamilies like myostatin and GDF11 [13,24,25]. In fact, recent characterization reveals that follistatin is an efficient inhibitor of myostatin and the closely related TGF-β family member, GDF11 [26]. Follistatin-related gene, called FLRG, was recently identified that has similar ligand binding specificity and structure as follistatin [27–29]. However, several differences between follistatin and FLRG should be noted. Follistatin has three follistatin domains, whereas FLRG only has two [20, 27–29]. Follistatin has a heparin-binding site in the first follistatin domain, whereas FLRG does not. In addition, FLRG immunolabeling was observed in the nuclei of several cell types [29,30]. Furthermore, transcriptional regulation of follistatin and FLRG is different [30,31]. Interestingly, myostatin and GDF11, whose affinity for follistatin is close to activin and higher than that of BMP ligands, shows activin-unique amino acid elements [23], indicating that myostatin and GDF11 are more closely related to activins. Proteomics analysis, to identify potential binding proteins for myostatin in human and mouse sera, yielded FLRG, myostatin propeptide, and a novel protein, GDF8-associating serum protein-1 (GASP-1), which also has a follistatin domain [32,33]. Thus, multiple proteins associate with myostatin *in vivo*.

Cerberus, DAN and gremlin have recently been identified as antagonists of BMP signaling [34]. Since BMP signaling plays a critical role in early embryogenesis, regulation of BMP signaling by the Cerberus/DAN family directly affects ventral/dorsal and anterior/posterior axis formation [35]. Noggin, unlike follistatin, forms an elongated homodimer (Fig. (**2**)). The crystal structure of noggin bound to BMP7 shows that noggin inhibits BMP7 signaling by blocking the molecular interfaces of the binding epitopes for both

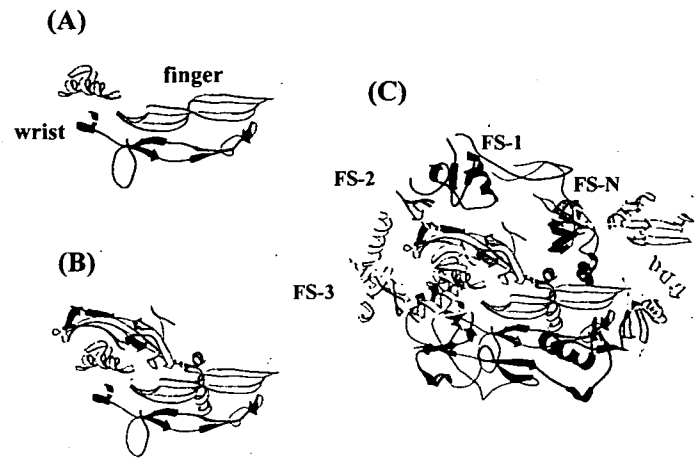

Fig. (1). Crystal structure of activin complexed with follistatin.

(A) Structure of an activin monomer is shown. The monomer shows a left-hand like structure including wrist and fingers. (B) Structure of activin dimer. The binding region for type I receptor is located near the wrist region, whereas the binding region for type II receptor is near the fingertips and knuckles. (C) Structure of activin dimer complexed with two molecules of follistatin. Follistatin adopts C-clamp-like conformations and encircles activin. Follistatin has four distinct domains, N-terminal domain (FS-N) and three follistatin (FS-1 to FS-3) domains. The follistatin N-terminal domain has a fold that occupies the type I receptor binding site. FS-1 and part of the FS-2 domains are involved in blocking the type II receptor binding site. The structure is from RCSB Protein Data Bank (PDB) 2B0U and displayed by using KiNG software. Alpha helix is shown in ribbon-like drawing, and beta strands are shown in specific colors.

type I and type II receptors [36] (Fig. (2)). Interestingly, the scaffold of noggin contains a cystine knot topology similar to that of the BMP family, suggesting that the ligand and its inhibitor may have evolved from a common ancestral gene by duplication [36] (Fig. (2)). The DAN family also has a cystine knot motif, indicating the importance of disulfide bondage to determine the three dimensional structure of BMP inhibitors.

Interestingly, ectodin, which belongs to the DAN/Cerberus family of BMP antagonists, is involved in mammalian tooth cusp patterning. Ectodin-deficient mice have enlarged enamel

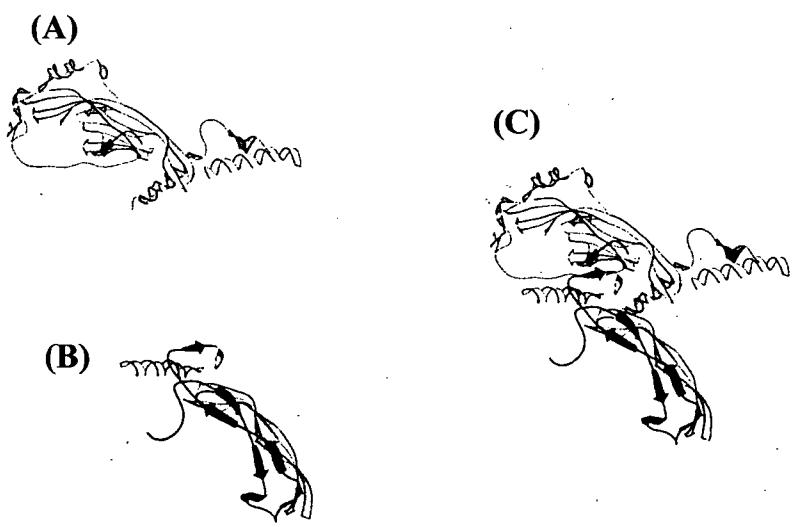

Fig. (2). Crystal structure of noggin and BMP7.

(A) Structure of noggin monomer. The scaffold of noggin has a cystine knot topology similar to BMP. Noggin forms a dimer with head-to-head contact, whereas BMP forms a dimer with head-to-tail interaction. (B) Structure of BMP7 monomer. (C) Structure of noggin monomer complexed with BMP7 monomer. Noggin inhibits BMP signaling by blocking the molecular interfaces of the binding epitopes for both type I and type II receptors. The structure is from PDB 1M4U and displayed by using KiNG software. Alpha helix is shown in ribbon-like drawing, and beta strands are shown in specific colors.

knots and extra teeth [37]. It is likely that excess BMP in ectodin-deficient teeth causes unchecked induction toward large enamel knots. Thus, modulation of ectodin would be useful for tooth regeneration.

Sclerostin is an osteocyte-derived negative regulator of bone formation [38]. The loss of sclerostin leads to sclerosteosis and Van Buchem disease characterized by high bone mass [39]. Sclerostin shows amino acid sequence similarity with the DAN family of BMP antagonists and was first hypothesized to act as a BMP antagonist [40]. However, recent characterization suggests that sclerostin binds low-density lipoprotein receptor-related proteins 5 and 6 (LRP5/LRP6) and could be a canonical Wnt inhibitor as well as a BMP antagonist [41,42]. Sclerostin is regarded as an attractive target for the development of bone formation therapy for diseases such as osteoporosis.

SMALL CHEMICAL TGF-β INHIBITORS

As a chemical TGF-β inhibitor, SB431542 was first reported as a selective inhibitor of TGF-β type I receptor kinase activity [43] (Fig. (3)). SB431542 is selective for inhibition of ALK4, 5 and 7 at low concentrations. Chemical TGF-β inhibitors may offer a novel option for cancer therapy by reducing cell proliferation, angiogenesis, motility, metastasis and fibrosis [44,45]. In addition to SB431542, SB505124 and A-83-01 have been developed [46,47]. A-83-01 was found to be more potent than SB431542 in the inhibition of TGF-β signaling [47]. The chemical inhibitors could be useful for preventing tumor progression and fibrosis in cases where TGF-β family members are involved. It is worthwhile noting that these compounds are not specific to TGF-βs, and inhibit activin, myostatin, GDF11 and nodal that signal through ALK4, 5 and 7.

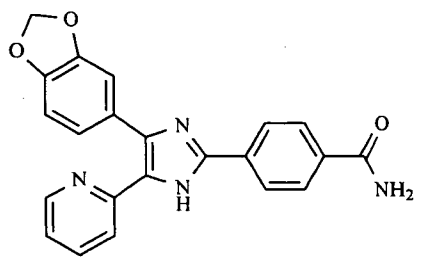

Fig. (3). Chemical structure of SB431542, 4-[4-(1,3-benzodioxol-5-yl)-5-(2-pyridinyl)-1H-imidazol-2-yl]benzamide, a specific inhibitor of TGF-β type I receptor kinase. Molecular formula of SB431542 is $C_{22}H_{16}N_4O_3$. Molecular weight of the compound is 384.39.

CANCER AND TGF-β INHIBITORS

As mentioned above, TGF-β has a dual role in tumor progression, both as a tumor suppressor and tumor promoter. Targeting a TGF-β tumor promoting activity is attractive since tumors are often resistant to the growth-inhibitory effect of TGF-β at the time of tumor detection. In particular, TGF-β plays an important role in promoting metastasis. In fact, one report showed that lifetime exposure to a soluble TGF-β antagonist protects against metastasis without adverse side effects [48]. Thus, it is predicted that inhibitors of the TGF-β signaling pathway would result in delays in tumor progression and improved survival (Table 1). Several clinical trials inhibiting TGF-β signaling by various strategies indicate that TGF-β inhibition may be a promising option for cancer therapy [2] (Table 1). Initially, the dominant negative form of TβRII was used to block TGF-β activity, and has been shown to prevent epithelial–mesenchymal transition [49]. Dominant negative TβRII also suppresses tumorigenicity and metastasis of thymoma and mammary tumors [50,51]. Antisense oligonucleotides against TGF-β are good clinical candidates for treatment of cancer and fibrosis [52] (Table 1). Monoclonal antibodies against TGF-β1 and β2, called lerdelimumab and metelimumab, respectively, have been developed and are now in phase II/III studies in nephropathy, fibrosis, glioblastoma, non-small cell lung carcinoma, and colorectal cancer [53,54] (Table 1). RNA interference technology to suppress expression of TGF-β and its receptors may offer an additional option for cancer therapy in the future [55]. As mentioned above, small chemical TGF-β inhibitors also have promising therapeutic potential.

MUSCULAR DISORDERS AND MYOSTATIN INHIBITORS

Skeletal muscle is affected in various muscle wasting conditions such as muscular dystrophy, neurogenic muscle atrophy, aging and disuse atrophy. Since skeletal muscle is the major target organ of insulin action, restoring skeletal muscle mass is favorable even in metabolic disorders, including diabetes mellitus and obesity [18]. Muscular dystrophies are intractable muscular diseases affecting skeletal muscles. Progressive muscle damage and muscle atrophy, infiltration of inflammatory cells in muscle and replacement of skeletal muscles with fibrous and fatty tissues are the hallmarks of the disease [18,56]. Although many of the genes responsible for the various types of muscular dystrophy have been investigated and identified by linkage analysis, effective therapies for muscular dystrophy have not yet become a reality. Theoretically, three major approaches i.e., gene therapy, cell therapy and drug therapy, have been tested with varying degrees of success. Myostatin, one of the TGF-β family of growth and differentiation factors, is a potent negative regulator of skeletal muscle growth and differentiation [13,57]. Regulation of myostatin activity determines skeletal muscle mass. Myostatin blockage is effective for an increase in muscle mass even in adults. Thus, myostatin is considered to be an excellent drug target for muscle wasting diseases such as muscular dystrophy. There are multiple strategies for inhibiting myostatin activity. Myostatin blocking antibody, myostatin propeptide, the soluble form of myostatin/activin receptor, and follistatin bind myostatin and block its action [18]. Indeed, antibody-mediated myostatin blockage in *mdx* mice, which is the model for Duchenne type muscular dystrophy, ameliorates the pathophysiology and muscle strength [58] (Table 1). Similarly, myostatin blockage and amelioration of *mdx* mice by myostatin propeptide were also reported [59,60]. How myostatin inhibition favors recovery from muscular dystrophy is not clear. It is hypothesized that balancing the muscle loss and atrophy caused by muscle wasting with increased muscle mass by myostatin blockage is beneficial for dystrophic muscles and may overcome muscle wasting [61]. Since TGF-β is involved in fibro-

Table 1. TGF-β Family Members and Their Inhibitors and Potential Clinical Applications

Ligand	Inhibitors			Applications
	Proteins	Antibodies & Antisense	Chemicals	
TGF-β	Decorin Soluble TGF-β receptor	lerdelimumab metelimumab AP-12009	SB431542 SB505124 A-83-01 LY550410	Cancer Fibrosis
Activin	Follistatin FLRG		SB431542 SB505124 A-83-01 LY550410	Cancer Fibrosis
Myostatin	Follistatin FLRG, GASP-1 GDF8 propeptide	MYO-029	SB431542 SB505124 A-83-01 LY550410	Muscular disorders
BMP	Noggin, chordin Cer/Dan, ectodin Sclerostin			Osteoporosis Teeth regeneration

sis in many organs, such as liver and kidney [45], and myostatin signaling is similar to that of TGF-β and activin, it is also likely that prevention of myostatin signaling is favorable for the prevention of fibrosis in muscular dystrophy. The biosafety and effectiveness of myostatin antibody MYO-029 is being evaluated in phase I/II studies in the United States in 108 patients suffering from muscular dystrophy [18]. In addition to myostatin antibody and myostatin propeptide, the soluble form of activin/myostatin receptor and follistatin are promising therapeutic tools for myostatin inhibition. The dominant negative form of activin type II receptor, ΔActRIIB, has a strong effect on increased skeletal muscle mass [26,62]. Also, skeletal muscle-targeted overexpression of follistatin causes strong increase of muscle mass [26]. Since ΔActRIIB and follistatin not only inhibit myostatin but also block the action of activin and GDF11, activin and GDF11 are also likely to control skeletal muscle differentiation and growth [4].

POTENTIAL APPLICATIONS OF BMP INHIBITORS

One of the major actions of BMP is ectopic bone formation. However, the actions of BMP are not confined to osteogenesis. BMP is involved in development of neurons, chondrogenesis, induction of apoptosis, and axis and mesoderm formation in early development. Multiple BMP inhibitors, including noggin, chordin and the Cerberus/Dan family, have been identified and characterized. Some of the inhibitors could have useful medical applications. In the field of dentistry, GDF11 has been characterized as possessing the ability to induce dental pulp stem cell differentiation into odontocytes. Accordingly, GDF11 could enhance the healing potential of pulp tissue [63]. Furthermore, mice deficient in BMP antagonist, ectodin, have enlarged enamel knots and extra teeth [37]. Therefore, tooth regeneration and healing after cavity treatment could be accelerated by regulating BMP/ectodin activity (Table **1**).

Osteoporosis is an important disease affecting morbidity and mortality in an aging world population. Current therapeutics includes inhibitors of osteoclast bone resorption, estrogenic compounds, bisphosphonates and parathyroid hormone [64]. Sclerostin works as a negative regulator of bone formation [39]. Thus, sclerostin is a novel drug target of osteoporosis (Table **1**).

PERSPECTIVES

Inhibitors for the TGF-β superfamily have great potential for multiple clinical applications. Inhibition of either TGF-β or activin could delay cancer progression and prevent fibrosis (Table **1**). Myostatin inhibition is a promising novel therapeutic strategy to treat muscular disorders, including muscular dystrophy (Table **1**). Targeting either BMP ligand or BMP inhibitors could be beneficial for osteoporosis and regeneration of bone and teeth (Table **1**).

Several molecules can inhibit TGF-β family members. Chemical inhibitors for the TGF-β family could be administered either intravenously or orally. Natural proteins and antibodies were intraperitoneally administered [10,58,60,62]. In the case of therapy of glioma, intracerebral and intrathecal infusion of antisense oligonucleotide has been trialed [65]. Since administered therapeutics degrade *in vivo*, frequent administration is needed. Conjugation/modification of antisense oligonucleotides, siRNA, chemicals and proteins with various compounds, such as polymers and nanoparticles, could prevent degradation before inhibitors for the TGF-β superfamily reach their target tissues and improve their delivery efficiency [66,67]. Even controlled and sustained release of potential therapeutics would be possible from microspheres embedded with hydrogels [67]. Development of TGF-β inhibitors and innovation of new technology for *in vivo* drug delivery will undoubtedly increase options for therapy against cancer and musculoskeletal disorders in which the TGF-β family plays a significant role.

ACKNOWLEDGEMENTS

This work was supported by a grant (16B-2) for Nervous and Mental Disorders, and a grant (17231401) for Research on Psychiatric and Neurological Diseases and Mental Health, both from the Ministry of Health, Labour and Welfare, a Grant-in-Aid for Scientific Research on Priority Areas from the Ministry of Education, Culture, Sports, Science and Technology (18052019), the Sankyo Foundation of Life Science, and SUZUKEN Memorial Foundation.

ABBREVIATIONS

TGF-β = Transforming growth factor-β

BMP = Bone morphogenetic proteins

DAN = Differential screening-selected gene aberrative in neuroblastoma

CDK = Cyclin-dependent kinase

ActRII = Activin type II receptor

ALK = Activin receptor-like kinase

GDF = Growth and differentiation factor

TβRII = TGF-β type II receptor

REFERENCES

[1] Siegel, P.M.; Massagué, J. *Nat. Rev. Cancer*, **2003**, *3*, 807.
[2] Tsuchida, K. *Curr. Drug Targets Immune Endocr. Metabol. Disord.*, **2004**, *4*, 157.
[3] Matsuura, I.; Denissova, N.G.; Wang, G.; He, D.; Long, J.; Liu, F. *Nature*, **2004**, *430*, 226.
[4] Iyer, S.; Wang, Z.G.; Akhtari, M.; Zhao, W.; Seth, P. *Cancer Biol. Ther.*, **2005**, *4*, 261.
[5] Nakamura, T.; Takio, K.; Eto, Y.; Shibai, H.; Titani, K.; Sugino, H. *Science*, **1990**, *247*, 836.
[6] Hempen, P.M.; Zhang, L.; Bansal, R.K.; Iacobuzio-Donahue, C.A.; Murphy, K.M.; Maitra, A.; Vogelstein, B.; Whitehead, R.H.; Markowitz, S.D.; Willson, J.K.; Yeo, C.J.; Hruban, R.H.; Kern, S.E. *Cancer Res.*, **2003**, *63*, 994.
[7] Su, G.H.; Bansal, R.; Murphy, K.M.; Montgomery, E.; Yeo, C.J.; Hruban, R.H.; Kern, S.E. *Proc. Natl. Acad. Sci. USA*, **2001**, *98*, 3254.
[8] Hahn, S.A.; Schutte, M.; Hoque, A.T.; Moskaluk, C.A.; da Costa, L.T.; Rozenblum, E.; Weinstein, C.L.; Fischer, A.; Yeo, C.J.; Hruban.,R.H.; Kern, S.E. *Science*, **1996**, *271*, 350.
[9] Eppert, K.; Scherer, S.W.; Ozcelik, H.; Pirone, R.; Hoodless, P.; Kim, H.; Tsui, L.C.; Bapat, B.; Gallinger, S.; Andrulis, I.L.; Thomsen, G.H.; Wrana, J.L.; Attisano, L. *Cell*, **1996**, *86*, 543.
[10] Adkins, H.B.; Bianco, C.; Schiffer, S.G.; Rayhorn, P.; Zafari, M.; Cheung, A.E.; Orozco, O.; Olson, D.; De Luca, A.; Chen, L.L.; Miatkowski, K.; Benjamin, C.; Normanno, N.; Williams, K.P.; Jarpe, M.; LePage, D.; Salomon, D.; Sanicola, M. *J. Clin. Invest.*, **2003**, *112*, 575.
[11] Bachman, K.E.; Park, B.H. *Curr. Opin. Oncol.*, **2005**, *17*, 49.
[12] Risbridger, G.P.; Schmitt, J.F.; Robertson, D.M. *Endocr. Rev.*, **2001**, *22*, 836.
[13] McPherron, A.C.; Lawler, A.M.; Lee, S.J. *Nature*, **1997**, *387*, 83.
[14] McPherron, A.C.; Lee, S.J. *Proc. Natl. Acad. Sci. USA*, **1997**, *94*, 12457.
[15] Schuelke, M.; Wagner, K.R.; Stolz, L.E. *N. Engl. J. Med.*, **2004**, *350*, 2682.
[16] Whittemore, L.A.; Song, K.; Li, X.; Aghajanian, J.; Davies, M.; Girgenrath, S.; Hill, J.J.; Jalenak, M.; Kelley, P.; Knight, A.; Maylor, R.; O'Hara, D.; Pearson, A.; Quazi, A.; Ryerson, S.; Tan, X.Y., Tomkinson, K.N.; Veldman, G.M.; Widom, A.; Wright, J.F.; Wudyka, S.; Zhao, L.; Wolfman, N.M. *Biochem. Biophys. Res. Commun.*, **2003**, *300*, 965.
[17] Grobet, L.; Pirottin, D.; Farnir, F.; Poncelet, D.; Royo, L.J.; Brouwers, B.; Christians, E.; Desmecht, D.; Coignoul, F.; Kahn, R.; Georges, M. *Genesis*, **2003**, *35*, 227.
[18] Tsuchida, K. *Expert Opin. Biol. Ther.*, **2006**, *6*, 147.
[19] Esparza-Lopez, J.; Montiel, J.L.; Vilchis-Landeros, M.M.; Okadome, T.; Miyazono, K.; Lopez-Casillas, F. *J. Biol. Chem.*, **2001**, *276*, 14588.
[20] Tsuchida, K.; Nakatani, M.; Matsuzaki, T.; Yamakawa, N.; Liu, Z.H.; Bao, Y.L.; Arai, K.Y.; Murakami, T.; Takehara, Y.; Kurisaki, A.; Sugino, H. *Mol. Cell. Endo.*, **2004**, 225, 1.
[21] Gumienny, T.L.; Padgett, R.W. *Trends. Endocr. Metab.*, **2002**, *13*, 295.
[22] Sugino, H.; Tsuchida, K. *Skeletal Growth Factor*, Lippincott Williams & Wilkins: Philadelphia, **2000**; pp. 251-263.
[23] Thompson, T.B.; Lerch, T.F.; Cook, R.W.; Woodruff, T.K.; Jardetzky, T.S. *Develop. Cell*, **2005**, *9*, 535.
[24] Matzuk, M.M.; Lu, N.; Vogel, H.; Sellheyer, K.; Roop, D.R.; Bradley, A. *Nature*, **1995**, *374*, 360.
[25] McPherron, A.C.; Lawler, A.M.; Lee, S.J. *Nat. Genet.*, **1999**, *22*, 260.
[26] Lee, S.J.; McPherron, A.C. *Proc. Natl. Acad. Sci. USA*, **2001**, *98*, 9306.
[27] Hayette, S.; Gadoux, M.; Martel, S.; Bertrand, S.; Tigaud, I.; Magaud, J.P.; Rimokh, R. *Oncogene*, **1998**, *16*, 2949.
[28] Tsuchida, K.; Arai, K.Y., Kuramoto, Y., Yamakawa, N.; Hasegawa, Y.; Sugino, H. *J. Biol. Chem.*, **2000**, *275*, 40788.
[29] Tortoriello, D.V.; Sidis, Y.; Holtzman, D.A.; Holmes, W.E.; Schneyer, A.L. *Endocrinology*, **2001**, *142*, 3426.
[30] Wang, H.Q.; Takebayashi, K.; Tsuchida, K.; Noda, Y. *J. Clin. Endo. Metab.*, **2003**, *88*, 4432.
[31] Liu, J.; Vanttinen, T.; Hyden-Granskog, C.; Voutilainen, R. *Mol. Hum. Reprod.*, **2002**, *8*, 992.
[32] Hill, J.J.; Davies, M.V.; Pearson, A.A.; Wang, J.H.; Hewick, R.M.; Wolfman, N M.; Qiu, Y. *J. Biol. Chem.*, **2002**, *277*, 40735.
[33] Hill, J.J.; Qiu, Y.; Hewick, R.M.; Wolfman, N.M. *Mol. Endocrinol.*, **2003**, *17*, 1144.
[34] Canalis, E.; Economides, A.N.; Gazzerro, E. *Endocr. Rev.*, **2003**, *24*, 218.
[35] Balemans, W.; Van Hul, W. *Dev. Biol.*, **2002**, *250*, 231.
[36] Groppe, J.; Greenwald, J.; Wiater, E.; Rodriguez-Leon, J.; Economides, A.N.; Kwiatkowski, W.; Affolter, M.; Vale, W.W.; Belmonte, J.C.; Choe, S. *Nature*, **2002**, *420*, 636.
[37] Kassai, Y.; Munne, P.; Hotta, Y.; Penttila, E.; Kavanagh, K.; Ohbayashi, N.; Takada, S.; Thesleff, I.; Jernvall, J.; Itoh, N. *Science*, **2005**, *309*, 2067.
[38] Ott, S.M. *J. Clin. Endocrinol. Metab.*, **2005**, *90*, 6741.
[39] Loots, G.G.; Kneissel, M.; Keller, H.; Baptist, M.; Chang, J.; Collette, N.M.; Ovcharenko, D.; Plajzer-Frick, I.; Rubin, E.M. *Genome Res.*, **2005**, *15*, 928.
[40] Winkler, D.G.; Sutherland, M.K.; Geoghegan, J.C.; Yu, C.; Hayes, T.; Skonier, J.E.; Shpektor, D.; Jonas, M.; Kovacevich, B.R.; Staehling-Hampton, K.; Appleby, M.; Brunkow, M.E.; Latham, J.A. *EMBO J.*, **2003**, *22*, 6267.
[41] van Bezooijen, R.L.; Roelen, B.A.; Visser, A.; van der Wee-Pals, L.; de Wilt, E.; Karperien, M.; Hamersma, H.; Papapoulos, S.E.; ten Dijke, P.; Lowik, C.W. *J. Exp. Med.*, **2004**, *15*, 805.
[42] Li, X.; Zhang, Y.; Kang, H.; Liu, W.; Liu, P.; Zhang, J.; Harris, S.E.; Wu, D. *J. Biol. Chem.*, **2005**, *280*, 19883.
[43] Laping, N.J.; Grygielko, E.; Mathur, A.; Butter, S.; Bomberger, J.; Tweed, C.; Martin, W.; Fornwald, J.; Lehr, R.; Harling, J.; Gaster, L.; Callahan, J.F.; Olson, B.A. *Mol. Pharmacol.*, **2002**, *62*, 58.
[44] Hjelmeland, M.D.; Hjelmeland, A.B.; Sathornsumetee, S.; Reese, E.D.; Herbstreith, M.H.; Laping, N.J.; Friedman, H.S.; Bigner, D.D.; Wang, X.F.; Rich, J.N. *Mol. Cancer Ther.*, **2004**, *3*, 737.
[45] Liu, X.J.; Ruan, C.M.; Gong, X.F.; Li, X.Z.; Wang, H.L.; Wang, M.W.; Yin, J.Q. *Biotechnol. Lett.*, **2005**, *27*, 1609.
[46] DaCosta Byfield, S.; Major, C.; Laping, N.J.; Roberts, A.B. *Mol. Pharmacol.*, **2004**, *65*, 744.
[47] Tojo, M.; Hamashima, Y.; Hanyu, A.; Kajimoto, T.; Saitoh, M.; Miyazono, K.; Node, M.; Imamura, T. *Cancer Sci.*, **2005**, *96*, 791-800.
[48] Yang, Y.A.; Dukhanina, O.; Tang, B.; Mamura, M.; Letterio, J.J.; MacGregor, J.; Patel, S.C.; Khozin, S.; Liu, Z.Y.; Green, J.; Anver, M.R.; Merlino, G.; Wakefield, L.M. *J. Clin. Invest.*, **2002**, *109*, 1607.

[49] Oft, M.; Heider, K.H.; Beug, H. *Curr. Biol.*, **1998**, *8*, 1243.
[50] Won, J.; Kim, H.; Park, E.J.; Hong, Y.; Kim, S.J.; Yun, Y. *Cancer Res.*, **1999**, *59*, 1273.
[51] Muraoka, R.S.; Dumont, N.; Ritter, C.A.; Dugger, T.C.; Brantley, D.M.; Chen, J.; Easterly, E.; Roebuck, L.R.; Ryan, S.; Gotwals, P.J.; Koteliansky, V.; Arteaga, C.L. *J. Clin. Invest.*, **2002**, *109*, 1551.
[52] Kaminska, B.; Wesolowska, A.; Danilkiewicz, M. *Acta Biochim. Polonica*, **2005**, *52*, 329.
[53] Benigni, A.; Zoja, C.; Corna, D.; Zatelli, C.; Conti, S.; Campana, M.; Gagliardini, E.; Rottoli, D.; Zanchi, C.; Abbate, M.; Ledbetter, S.; Remuzzi, G.J. *Am. Soc. Nephrol.*, **2003**, *14*, 1816.
[54] Mead, A.L.; Wong, T.T.; Cordeiro, M.F.; Anderson, I.K.; Khaw, P.T. *Invest. Ophthal. Vis. Sci.*, **2003**, *44*, 3394.
[55] Friese, M.A.; Wischhusen, J.; Wick, W.; Weiler, M.; Eisele, G.; Steinle, A.; Weller, M. *Cancer Res.*, **2004**, *64*, 7596.
[56] Zammit, P.S.; Partridge, T.A. *Nat. Med.*, **2002**, *8*, 1355.
[57] Lee, S.-J. *Annu. Rev. Cell. Dev. Biol.*, **2004**, *20*, 61.
[58] Bogdanovich, S.; Krag, T.O.; Barton, E.R.; Morris, L.D.; Whittemore, L.A.; Ahima, R.S.; Khurana, T.S. *Nature*, **2002**, *420*, 418.
[59] Nishi, M.; Yasue, A.; Nishimatu, S.; Nohno, T.; Yamaoka, T.; Itakura, M.; Moriyama, K.; Ohuchi, H.; Noji, S. *Biochem. Biophys. Res. Commun.*, **2002**, *293*, 247.
[60] Bogdanovich, S.; Perkins, K.J.; Krag, T.O.; Whittemore, L.A.; Khurana, T.S. *FASEB J.*, **2005**, *19*, 543.
[61] Khurana, T.S.; Davies, K.E. *Nat. Rev. Drug. Discov.*, **2003**, *2*, 379.
[62] Lee, S.J.; Reed, L.A.; Davies, M.V.; Girgenrath, S.; Goad, M.E.; Tomkinson, K.N.; Wright, J.F.; Barker, C.; Ehrmantraut, G.; Holmstrom, J.; Trowell, B.; Gertz, B.; Jiang, M.S.; Sebald, S.M.; Matzuk, M.; Li, E.; Liang, L.F.; Quattlebaum, E.; Stotish, R.L.; Wolfman, N.M. *Proc. Natl. Acad. Sci. USA*, **2005**, *102*, 18117.
[63] Nakashima, M.; Mizunuma, K.; Murakami, T.; Akamine, A. *Gene Ther.*, **2002**, *9*, 814.
[64] Grey, A.; Reid, I.R. *Expert Opin. Investig. Drugs*, **2005**, *14*, 265.
[65] Schlingensiepen, R.; Goldbrunner, M.; Szyrach, M.N.; Stauder, G.; Jachimczak, P.; Bogdahn, U.; Schulmeyer, F.; Hau, P.; Schlingensiepen, K.H. *Oligonucleotides*, **2005**, *15*, 94.
[66] Sirsi, S.R.; Williams, J.H.; Lutz, G.J. *Hum. Gene Ther.*, **2005**, *16*, 1307.
[67] DeFail, A.J.; Chu, C.R.; Izzo, N.; Marra, K.G. *Biomaterials*, **2006**, *27*, 1579.

Received: April 21, 2006 **Revised: May 19, 2006** **Accepted: May 20, 2006**

Expert Opinion

Peptides, Proteins & Antisense

The role of myostatin and bone morphogenetic proteins in muscular disorders

Kunihiro Tsuchida
Institute for Comprehensive Medical Science (ICMS), Division for Therapies against Intractable Diseases, Fujita Health University, Toyoake, Aichi 470-1192, Japan

Skeletal muscle is the largest organ in the human body, and plays an important role in body movement and metabolism. Skeletal muscle mass is lost in genetic disorders such as muscular dystrophy, muscle wasting and ageing. Chemicals and proteins that restore muscle mass and function are potential drugs that can improve human health and could be used in the clinic. Myostatin is a muscle-specific member of the transforming growth factor (TGF)-βsuperfamily that plays an essential role in the negative regulation of muscle growth. Inhibition of myostatin activity is a promising therapeutic method for restoring muscle mass and strength. Potential inhibitors of myostatin include follistatin domain-containing proteins, myostatin propeptide, myostatin antibodies and chemical compounds. These inhibitors could be beneficial for the development of clinical drugs for the treatment of muscular disorders. Bone morphogenetic protein (BMP) plays a significant role in the development of neuromuscular architecture and its proper functions. Modulation of BMP activity could be beneficial for muscle function in muscular disorders. This review will describe the current progress in therapy for muscular disorders, emphasising the importance of myostatin as a drug target.

Keywords: BMP, disuse atrophy, follistatin, muscular dystrophy, myostatin, neuromuscular junction

Expert Opin. Biol. Ther. (2006) 6(2):147-154

1. Introduction

Skeletal muscle is the largest organ in the human body and is affected in myogenic, neurogenic and metabolic disorders. Skeletal muscles become atrophic by muscular disorders such as muscular dystrophy, wasting, ageing and disuse atrophy. Neuronal innervation is required for skeletal muscle, and muscles become atrophic when motor neurons are affected by neurodegenerative disorders such as amyotrophic lateral sclerosis (ALS). Skeletal muscles are targets of insulin action, and muscle dysfunction is related to the pathogenesis of diabetes mellitus and obesity.

Restoring muscle mass and function lost by genetic disorders such as muscular dystrophy, neurodegenerative disorders and diabetes is important for human health. Myostatin is a potent negative regulator of skeletal muscle growth and differentiation [1,2]. Myostatin is considered to be a good drug target for muscular disorders, and myostatin blockage is one of the promising therapies for muscular dystrophy and myosarcoma. Bone morphogenetic proteins (BMPs), like myostatin, are members of the transforming growth factor (TGF)-β superfamily. BMPs play a specific role in bone growth and muscle development. Deciphering the precise roles of myostatin and BMPs is essential for understanding pathogenesis and devising a realistic therapy for intractable muscular disorders [1-3].

Ashley Publications
www.ashley-pub.com

2. The role of myostatin/BMPs in the development and growth of skeletal muscle

Development and growth of skeletal muscles are regulated by myostatin. During embryogenesis, skeletal muscles are formed from somites. Myostatin is initially expressed in the myotome layer of somites that gives rise to skeletal muscle, and this expression restricts muscle growth [4]. Mice lacking the myostatin gene have a 25 – 30% increased muscle mass [5]. Both muscle hyperplasia and hypertrophy were observed in the muscle fibres of mutant mice [5]. Several spontaneous mutations of the myostatin gene have been found in cattle that had doubling muscle phenotypes [6]. Interestingly, a child who had a splice site mutation in the myostatin gene displayed muscle hypertrophy [7]. This indicates that myostatin regulates muscle growth in humans as well as in mice and cattle. Myostatin is produced mainly by skeletal muscle in the adult. Like endocrine hormones, myostatin circulates in the serum in high amounts [8] and limits muscle fibre growth. Blockage of myostatin function, even in adult mice, using a myostatin antibody or conditional knockout technology resulted in an increase in muscle mass [9,10].

Skeletal muscle consists of two major fibre types: slow-twitch oxidative type I fibre and fast-twitch glycolytic type II fibre. Fibre composition is regulated by neuronal innervation and physical activity, and is altered in pathological conditions. The observation that the percentage of type I fibres was lower in myostatin-deficient cattle compared with normal cattle suggests that myostatin controls the relative ratio of type I fibre and type II fibre [11].

BMP, as its name implies, has been better recognised as an essential regulator of osteogenesis. BMPs stimulate osteoblast differentiation, but inhibit myogenic differentiation of myoblasts. Osteogenesis and myogenesis take place at adjacent sites and influence each other. The timing and location of myogenesis within the somite is controlled by relative levels of BMP activity and localised expression of BMP antagonists [12].

Skeletal muscles communicate with neurons through synapses at the neuromuscular junctions (NMJs) during development. Essential molecules for muscle function, such as acetylcholine receptors, accumulate in the postsynaptic membrane in adult skeletal muscles (Figure 1) [13]. Both retrograde and orthograde signals between neurons and muscles are required to coordinate synaptic development [13]. There is accumulating evidence that retrograde BMP signals from muscles influence NMJ development [14].

Generation of motor neurons, sensory neurons and interneurons in the spinal cord is regulated by specific BMP members and activins [4]. Namely, the fate of the dorsal region of the neural tube is established by the concentration gradient of BMP and activins, both of which are members of the TGF-β superfamily [4]. Initially, BMP4 and BMP7 are expressed in the epidermis, which serves as a second signalling centre by inducing BMP4 expression in the roof plate of the neural tube. Then, BMP4 from the roof plate induces a gradient of the TGF-β superfamily, such as BMP9 and activin, in adjacent cells. Different subsets of cells are exposed to different concentrations of each member of the TGF- superfamily at different developmental time points. The temporal and spatial concentration gradients of BMP and activins are responsible for inducing different sets of transcription factors in cells, thereby giving them different cell identities, including motor neurons innervating skeletal muscles [4].

3. Diseases affecting muscles

3.1 Muscular dystrophy

The muscular dystrophies are representative intractable neuromuscular disorders [1-3]. The most common type is Duchenne muscular dystrophy (DMD). In addition, a milder form called Becker muscular dystrophy (BMD), facioscapulohumeral muscular dystrophy (FSHD) and multiple types of limb girdle muscular dystrophy (LGMD) are known. Progressive muscle damage, muscle atrophy, tissue inflammation, and replacement of normal muscle fibres with fibrous tissues result in muscle wasting in muscular dystrophy. Dystrophin was identified as the gene responsible for DMD. Since then, many genes for various types of muscular dystrophy have been identified [15,16]. Most of the defective gene products are components of the dystrophin–glycoprotein complex protecting the skeletal muscle membrane from damage (Figure 1).

Muscular dystrophy is the focus of three different supportive or therapeutic approaches: gene therapy, cell therapy and drug therapy. Gene therapies that aim to replace the defective genes have been tried with various degrees of success for muscular dystrophy. Gene transfer methodologies, such as exon-skipping of the dystrophin gene and adeno-associated viruses, have advanced recently [16]. Cell transplantation research for skeletal muscles has also greatly advanced. Multiple myogenic precursor cells, including satellite cells residing near muscle fibres, bone marrow side population cells and mesoangioblasts, have been identified as myogenic stem cells. Cell therapy using mesoangioblasts, a class of vessel-associated stem cells, is one of the most promising therapeutic methods for muscular dystrophy [17].

Pharmacological drug strategies are also trialled [15,16]. Cycles of degeneration and regeneration of skeletal muscles take place under both normal use and pathological conditions. Corticosteroids, creatine and an inhibitor of prostaglandin synthesis are candidates for the treatment of dystrophy [15]. In addition, proteins and chemicals that increase muscle mass are quite promising for the treatment of muscular dystrophy, as extreme muscle loss and atrophy are the most prominent signs of the disease. One type of positive growth factor for myoblast proliferation is insulin-like growth factor (IGF). By contrast, myostatin is a potent negative growth regulator of muscle growth. Thus, enhancing IGF action or inhibiting myostatin activity would be favourable for muscle-progenitor proliferation and for increasing muscle mass. Indeed, IGF-1 has been shown to increase muscle mass and improve the

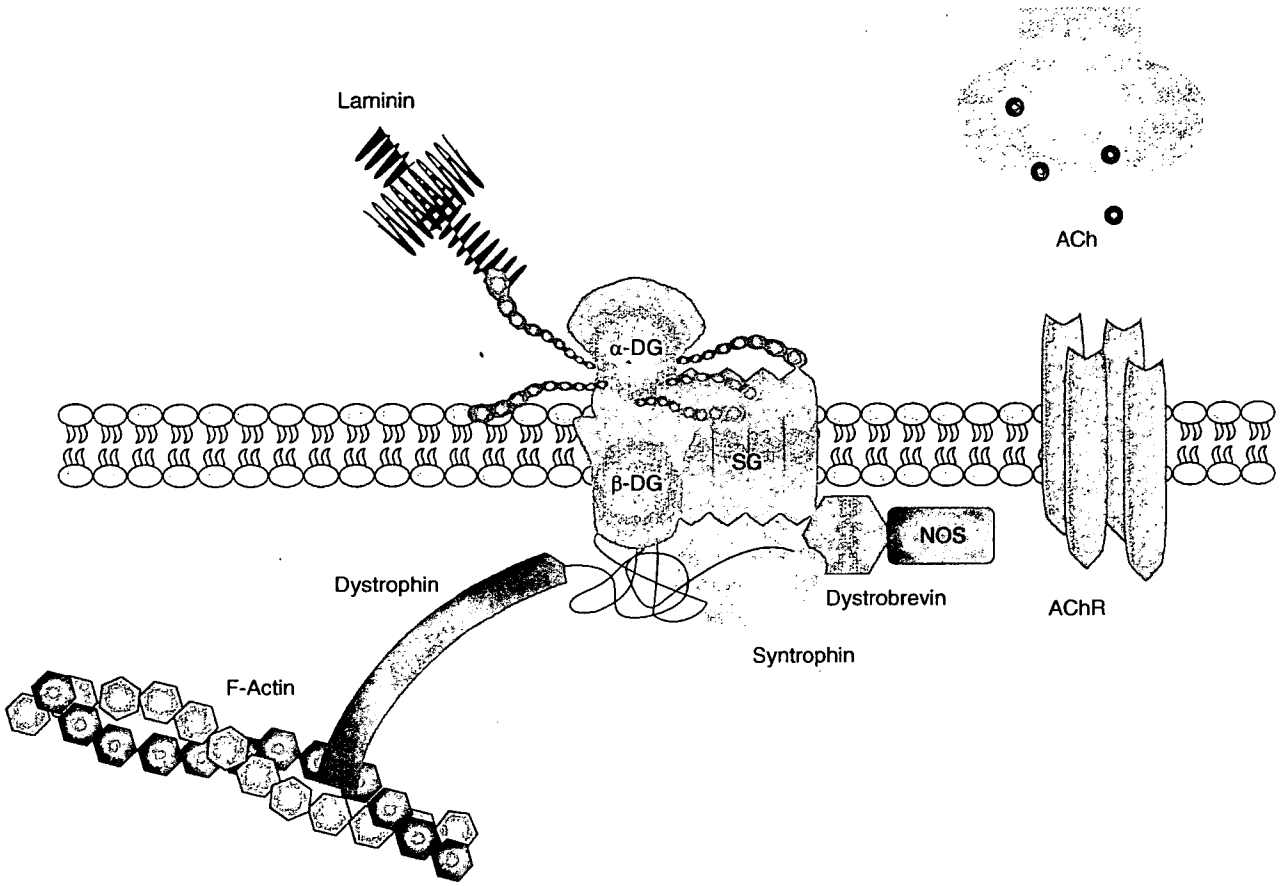

Figure 1. Schematic representation of neuromuscular junctions and dystrophin–glycoprotein complex. Dystrophin links cytoskeletal actin to the extracellular matrix via a dystrophin–glycoprotein complex. This complex consists of dystroglycans (and), sarcoglycans, syntrophins, dystrobrevins and NOS. Acetylcholine secreted from nerve terminals of motor neurons activates acetylcholine receptors located at plasma membranes of skeletal muscles.
Ach: Acetylcholine; AChR: Acetylcholine receptor; DG: Dystroglycan; NOS: Nitric oxide synthetase; SG: Sarcoglycan.

disease phenotype in *mdx* mice [18]. Similarly, as myostatin blockage is effective for an increase in muscle mass, even in adults, myostatin inhibition is also promising as a treatment for dystrophy [19-21]. Myostatin associates with a number of peptide hormones *in vivo*. Follistatin, follistatin-related gene (FLRG), follistatin-domain containing protein and myostatin prodomain peptide all bind myostatin and block myostatin activity [1,2,8,22,23]. Myostatin signals through a combination of activin type II receptors (ActRIIB and ActRIIA) and activin receptor-like kinases (ALKs) 4 and 5 [24]. Thus, myostatin could be inhibited by various approaches, including dominant-negative activin receptors, follistatin, follistatin domain-containing proteins and myostatin antibodies [1,2,8,22]. Recently, antibody-mediated myostatin blockage in *mdx* mice was used to improve dystrophy [19]. Blocking myostatin in *mdx* mice not only increased the number of normal muscle cells, but also augmented muscle strength. Myostatin propeptide-mediated amelioration of *mdx* mouse pathophysiology has recently been reported [21]. These data clearly indicate that myostatin inhibition is a promising therapy for muscular dystrophy. The mechanism by which myostatin blockage resulted in the recovery of muscle function is not clear, but it is proposed that balancing the muscle loss by wasting with increased muscle mass by myostatin blockage would be beneficial for dystropic muscles and overcome muscle wasting [3]. Follistatin and FLRG are the most potent molecules in inhibiting myostatin activity. Follistatin is better known as a high-affinity activin-binding protein [1,25,26]. Gene disruption of follistatin shows multiple defects, including muscle loss and rib abnormalities, indicating that follistatin can not only interact with activins, but also with other members of the TGF-β superfamily, notably with myostatin and GDF11 [27]. Indeed, follistatin showed a high affinity with myostatin *in vitro* [22]. The regions of activin important for follistatin binding have been mapped and were found to overlap with the region for activin essential for binding to the activin receptor [28]. Knowledge of the precise follistatin-binding regions in activin and myostatin would be of great help for understanding the structure requirement of myostatin inhibitors. In addition to follistatin, FLRG has been identified